NASA TECHNICAL NOTE

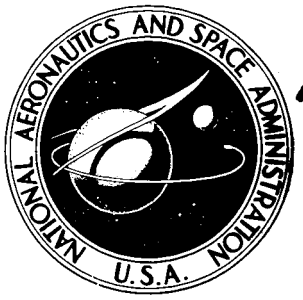

NASA TN D-7160

NASA TN D-7160

SOME EFFECTS OF WING PLANFORM ON SONIC BOOM

by Lynn W. Hunton, Raymond M. Hicks, and Joel P. Mendoza

Ames Research Center
Moffett Field, Calif. 94035

NATIONAL AERONAUTICS AND SPACE ADMINISTRATION • WASHINGTON, D. C. • JANUARY 1973

1. Report No.	2. Government Accession No.	3. Recipient's Catalog No.
NASA TN D-7160		

4. Title and Subtitle	5. Report Date
SOME EFFECTS OF WING PLANFORM ON SONIC BOOM	January 1973
	6. Performing Organization Code

7. Author(s)	8. Performing Organization Report No.
Lynn W. Hunton, Raymond M. Hicks, and Joel P. Mendoza	A-4491
	10. Work Unit No. 136-13-02-01-00-21
9. Performing Organization Name and Address	11. Contract or Grant No.
NASA Ames Research Center Moffett Field, Calif., 94035	
	13. Type of Report and Period Covered
12. Sponsoring Agency Name and Address	Technical Note
National Aeronautics and Space Administration Washington, D. C., 20546	14. Sponsoring Agency Code

15. Supplementary Notes

16. Abstract

A wind-tunnel investigation was conducted to determine the effect of wing planform on sonic boom at Mach numbers of 1.7, 2.0, and 2.7. The results of the investigation show that the wing leading-edge sweep is one of the primary planform variables affecting the overpressure characteristics.

17. Key Words (Suggested by Author(s))	18. Distribution Statement
Overpressure Sonic boom Wing planform Shock Pressure field	Unclassified – Unlimited

19. Security Classif. (of this report)	20. Security Classif. (of this page)	21. No. of Pages	22. Price*
Unclassified	Unclassified	39	$3.00

* For sale by the National Technical Information Service, Springfield, Virginia 22151

NOMENCLATURE

c	wing chord
C_L	lift coefficient
$F(\tau)$	$\frac{1}{2}\pi\int\left(\frac{2}{\beta R(t)}\right)^{1/2} H\left(\frac{\tau-t}{\beta R(t)}\right) dS'(t)$
h	altitude
H	Heaviside step function
l	reference body length
M	Mach number
p	reference pressure
Δp	sonic boom overpressure
r	body radius
$R(t)$	radius of equivalent body of revolution
$S'(t)$	first derivative of area distribution
t	wing thickness or dummy variable for length
x	distance along body axis
Δx	distance along abscissa of pressure signature
y	distance along wing semispan
β	$(M^2-1)^{\frac{1}{2}}$
τ	distance along abscissa of F–function
τ_o	value of τ where $\int_o^\tau F(t)dt$ is maximum

SOME EFFECTS OF WING PLANFORM ON SONIC BOOM

Lynn W. Hunton, Raymond M. Hicks, and Joel P. Mendoza

Ames Research Center

SUMMARY

A general research program was conducted to investigate, analytically and experimentally, the overpressure characteristics of conventional and unconventional wing planform shapes at Mach numbers of 1.7, 2.0, and 2.7. Twelve different planforms including a delta wing series, a swept wing series, and a curved leading-edge wing series were studied.

The results of the investigation show that the effect of wing leading-edge sweep angle on the level of sonic-boom overpressure is as large as the effect of other wing planform geometry changes (e.g., cranked or curved leading edge, tandem wings, etc.), both in the near field and at flight altitude.

A comparison of the experimental pressure signatures with Whitham-Lighthill theory shows that the degree of correlation depends primarily on configuration slenderness and the distance ratio from the flight path. Planform complexity appears to have little bearing on the agreement between experiment and theory.

INTRODUCTION

Ultimate public acceptance of mass transportation at supersonic speeds will be influenced to a large extent by the effectiveness of the solutions that can be found to the sonic-boom noise problem. While criteria defining the specifics of the maximum acceptable overpressure remain to be established, basic research in sonic-boom is continuing (see refs. 1 to 3 for a summary) in an effort to find effective design methods for reducing the overpressure and impulse from supersonic aircraft to the lowest possible levels.

Much of the early research undertaken on boom suppression has been directed at optimization studies (refs. 4 to 7) of the longitudinal distribution of cross-sectional area of simple (single-arc) axisymmetric bodies. In a recent application of an optimization search technique to the overpressure problem (ref. 8), other optimum bodies of revolution composed of multiple arcs were found to offer potential improvements. Justification for the use of favorable body shaping as a guideline in the design of lifting airplanes is based on the concept of equivalence of areas for volume and lift found in the supersonic area rule derived by Hayes (ref. 9), Jones (ref. 10), and Lomax (ref. 11). Use of this equivalent area concept in the design of an airplane configuration to achieve a target overpressure level (given weight, Mach number, and distance ratio) requires a fairly accurate prediction of the lift distribution. Since the available calculation methods for sonic boom and loading (e.g., refs. 12 and 13, respectively) are based on linearized theory that entails slender-body assumptions, pertinent questions arise regarding the reliability of these methods for analyzing

configurations where the effective slenderness is compromised by the addition of lift and high Mach number effects. Consequently, any realistic research program on the sonic-boom problem necessitates a constant integration of the results of theory with experiment if valid solutions are to be found.

In support of a general research program on sonic-boom suppression, an investigation was undertaken at Ames Research Center of a number of wing-body configurations to provide (1) an assessment of the available theory for predicting overpressure characteristics of arbitrary lifting configurations to Mach 2.7 and (2) a study of unconventional lifting configurations to gain new insight into potential shock-suppression techniques that have gone unrecognized in earlier theoretical analyses. While numerous correlations of theory and experiment have been conducted in the past (e.g., refs. 14 to 16), these correlations, for the most part, have been restricted to the lower Mach numbers and to conventional wing-body shapes. The study reported here deals particularly with the effect of wing planform shape on the overpressure characteristics for lift coefficients to about 0.2. Twelve different wings having a constant wetted area and volume in combination with a fixed body were tested in the Ames 9- by 7- foot and 8- by 7- foot supersonic wind tunnels at Mach numbers of 1.68, 2.0, and 2.7.

MODELS

The twelve models investigated in this study (fig. 1) include three classes of wing planforms covering delta, swept, and curved leading-edge types. As shown in the figure, the delta series has both conventional and tandem wing arrangements. In the design of the models, the fuselage dimensions and the total wetted area were held constant for all models except number 12. All wings had double-wedge 5-percent-thick sections with the ridge line located at midchord and were mounted on the cylindrical portion of the fuselage at the longitudinal plane of symmetry. As shown in figure 1, the bodies were the same for all configurations tested, having a fineness ratio (l/d) of 16.2 and a parabolic nose as described in the figure. All models were constructed of steel.

APPARATUS AND TESTS

Figure 2 is a sketch of the wind-tunnel test apparatus. The linear actuator mounted on the tunnel model support strut provided a remote control of the longitudinal position (62.5 cm travel) of the model with respect to two pressure probes fixed on the tunnel wall. The static probes were slender cones with an included angle of 2°. Four pressure orifices were located at 90° intervals around the circumference of each probe. The orifices of the reference probe were in a plane normal to the free stream while those for the overpressure probe were oriented in a plane parallel to the Mach angle for Mach 1.68. This procedure produces a sharper near-field signature. The distance of the model from the probe and the model angle of attack were remotely controllable. Model normal force was measured by an internal strain-gage balance.

The investigation was conducted in the Ames 9- by 7- foot and 8- by 7- foot supersonic wind tunnels; figure 3 is a photograph of the test setup in the 9- by 7- foot test section. Overpressure

measurements for the models were made at Mach numbers of 1.68, 2.0, and 2.7 in the vertical plane of symmetry at distance ratios (h/l) of 3.6, 2.6, and 3.1, respectively. The test stagnation pressure was 103,400 N/m^2 (15 psia) at all Mach numbers.

THEORETICAL METHODS

The sonic-boom computer program used at Ames Research Center was developed to give the capability of determining the contribution of each airplane component, including lift, to the total sonic-boom level. It is necessary therefore to calculate the F-function separately for each airplane component, including lift, and to sum the various F-functions to obtain the total F-function.

The F-functions for the body, body wake, and sting were computed using the nonsmooth form of the F-function (eq. (21) of ref. 12). The body wake was simulated by a 12° truncated cone. This treatment is identical to that of the wake of the 5-10 calibre ogival-head bullet in reference 12. The sting was included in the F-function calculation to define the characteristics of the rear shock. The cross-sectional area distributions due to volume for each of these items were developed by cutting planes normal to the body axis. This procedure is justified since the effect of Mach number is included in the integrand of the Whitham-Lighthill integral.

The individual F-functions for the wing thickness and the lift were computed using the smooth slender-body form of the F-function (eq. (14) of ref. 12). The wing cross-sectional area distribution was developed by cutting planes parallel to the free-stream Mach lines for each test Mach number using the wave drag computer program of reference 17. The lift distribution was computed by integrating the surface pressures calculated by the Ames Finite-Element Wing-Body Aerodynamics Computer program (ref. 13).

RESULTS AND DISCUSSION

Presentation of Results

The experimental and theoretical pressure signatures for the models at three values of lift coefficient are shown in figures 4 through 9 for test Mach numbers of 1.68, 2.00, and 2.70. Included in the figures are extrapolated signatures derived from the experimental and theoretical results for midfield distance ratios. Only at Mach 1.68 was the complete set of 12 models investigated. For this study, the bow shock of the theoretical pressure signature is located at the origin ($\Delta x/l = 0$) and the experimental signature is arbitrarily aligned with the theoretical signature at τ_O. This positioning of the signatures provides a more direct correlation of experiment with theory.

Comparison of Theory With Experiment

General observations– The use of current sonic-boom theory to predict the near-field pressure signature of complex aircraft configurations is questionable, particularly for lifting configurations and increasing Mach number. Calculations of the pressure signature and shock-wave pattern in the flow field surrounding an arbitrary aircraft configuration have been based almost exclusively on the supersonic projectile theory of Whitham (ref. 12) and the supersonic area rule of Hayes (ref. 9) and Lomax (ref. 11). The supersonic area rule indicates that the three-dimensional pressure field surrounding a complex lifting configuration can be approximated by that produced by an equivalent body of revolution. Experience has shown that this equivalence is accurate only when applied to slender configurations and only at large distances from the body where the three-dimensional effects of the flow field have almost disappeared. Further, the selection of the equivalent body of revolution requires knowledge of the distribution of the lift on the original body, usually determined from linear (potential) aerodynamic theory. Woodward (ref. 18) points out the difficulty of determining the lift distribution for low-aspect-ratio wings with supersonic leading edges. Available calculation methods based on linearized theory cannot adequately define the flow-field interactions of the three-dimensional tip region with the two-dimensional region behind the supersonic leading edge. However, regardless of the limitations of the theory, the wave pattern in the very near field is of interest in the phase of sonic-boom research dealing with the development of aircraft shapes for low boom since it is in this region that the interactions of the pressure waves from the various components of the airplane occur. The resulting reinforcement or cancellation of the waves in the near-field ultimately determines the level of the far-field pressure signature. Since the equivalent body concept may not be applied in the near-field region, research on overpressure characteristics at near-field distances must therefore rely heavily on experimental results with particular attention to testing techniques.[1]

While the importance of the near-field signature from a research standpoint is recognized for the reasons cited, a final assessment of the overpressure and impulse characteristics of a given configuration must be based ultimately on the midfield signature obtained by extrapolating [2] the near-field data to the distance ratio appropriate for the supersonic mission under consideration. In general, the degree of correlation between theory and experiment at the flight distance ratio will depend on the type of signature found. A near-field-type signature often shows a poor correlation whereas a far-field-type (N-wave) signature usually shows a good correlation.

Lift and Mach number effects– With the body geometry fixed for all models, the body bow-shock overpressures, with two exceptions, remain fairly constant with change of wing configuration as expected (see figs. 4–9). The exceptions are the configurations having tandem wings (models 2 and 3 in figs. 4(b), 4(c), 8(b), and 8(c)). Near zero lift at all three test Mach numbers, the

[1] An alternative approach is being developed by Kutler and Lomax (ref. 19). Their method is based on a numerical solution of the three-dimensional supersonic flow field which allows for all essential nonlinear effects and provides a determination of the complete near flow field.

[2] The need for near-field signature measurements in the wind tunnel together with the computational methods for performing the extrapolation were first proposed by Hicks and Mendoza (ref. 20) with later supplements appearing in references 21 and 22. An improved extrapolation procedure has recently been formulated by Thomas (ref. 23).

calculated shock overpressures for the near-field condition show generally good agreement with experiment at the body nose, whereas the agreement at the wing leading edge is somewhat less consistent. The discrepancies in the region of the wing appear due to an underprediction of the effective equivalent area for wing thickness and to a tendency of the Whitham theory to overcorrect the location of the characteristics. These effects lead to an underprediction of the pressure expansion slopes and to poor agreement between theory and experiment for the shock locations, signature lengths, and impulse characteristics. These zero lift thickness discrepancies also increase as slenderness is reduced either in the configuration (e.g., compare swept wing, fig. 5(a), with the trapezoidal wing, fig. 6(a), or with an increase in Mach number (e.g., compare M 1.68, fig. 4(a) with M 2.7, fig. 8(a) for the delta wing).

With the addition of lift, the discrepancies between theory and experiment intensify. Here the signature correlations are found to depend on the coalescence characteristics of the bow and wing-shock systems. For a near-field-type signature, the magnitude of the shock pressure peaks was predicted reasonably well (see figs. 4–7, 8(b), 8(c)). However, for the cases with shocks coalesced to an N-wave, the resulting predictions of shock-pressure peaks are in error by as much as 40 percent (e.g., see figs. 8(a), 8(d), and 9). As for zero lift, discrepancies occur in the shock locations, expansion slopes, and impulses regardless of the accuracy of the predicted shock-pressure peaks. Carlson, McLean, and Shrout (ref. 24) have proposed corrections to account for configuration angle-of-attack effects. While the theoretical data presented here have not been corrected in this manner, such an adjustment should improve the correlations under lifting conditions. In these tests, while the magnitude of the lift on the model was quite accurately measured by an internal strain-gage balance, the distribution of lift was not known. It is quite likely, therefore, that the discrepancies in calculated effects of lift can be attributed in some measure to the limitations of supersonic lifting theory as well as to sonic-boom theory in the near field. Until models large enough to permit the measurement of the load distributions are tested, the details of these limitations in theory cannot be resolved.

Note that the pressure data downstream of the tail shock for all configurations tested at Mach 2.70 show evidence of interference from the support sting for the lifting condition at $C_L = 0.15$ to 0.16 (see figs. 8 and 9). No attempt was made to correct the data.

Theoretical and extrapolated experimental pressure signatures are included in figures 4 to 8 for each model for distance ratios of 130 for Mach 1.68, 160 for Mach 2.0, and 200 for Mach 2.7. The values of distance ratio were varied with Mach number to approximate the altitude requirements of an assumed supersonic transport mission covering two climb conditions and one cruise condition. The extrapolation procedure used here (described in ref. 20) does not include the real atmosphere effects on shock coalescence as derived recently by Hayes, Haefeli, and Kulsrud (ref. 25) or Thomas (ref. 23). Insufficient pressure signature data were obtained downstream of the tail shock to permit extrapolations of the experimental tail shock region to the flight distance ratios assumed here. Hence, only theory will be found on the plots for the tail shock region. In addition, note the two data plots (figs. 6(a) and 7) where the theoretical calculations and experimental signature extrapolations were conducted for values of lift coefficient slightly different than indicated for the measured data. For these cases, all necessary interpolations were performed to correct the extrapolated signature to the lift coefficient indicated.

Near zero lift, the experimental signature extrapolation tended to predict shock pressure peaks about 10 percent higher than theory at Mach 1.68 and about 25 percent higher at Mach 2.7.

Contributing to this difference was a tendency of the theory to predict an expansion to lower pressure levels behind the bow shock compared to experiment, thereby reducing the coalescence of the wing and bow shocks for the theoretical signatures.

At higher lift coefficients, the deficiencies of theory mentioned above appear to continue, leading to percentage discrepancies of about the same level as just noted. However, exceptions to this generalization for several of the planforms will be noted further in the discussion of planform effects. The large discrepancies between theory and experiment found in the near-field at about $C_L = 0.15$ disappear almost entirely at the flight distance ratios for some configurations (see fig. 8). The degree of correlation found between theory and experiment at the flight distance ratio appears to depend to some extent on the strength of the wing shock in relation to that of the bow shock. Thus, a near-field signature containing a wing shock 50 to 100 percent greater (depending on Mach number) than the bow shock will quickly develop the characteristics of a far-field N-wave and, hence, the correlation between theory and experiment is good. Conversely, where the wing-shock strength is near that of the bow shock, the coalescence of the two shocks will be greatly reduced or, in some cases, even terminated. In this case, theory and experiment do not agree as well (see figs. 4(b) and 4(c)). This shock coalescence phenomenon has been examined quite extensively at Ames Research Center as a potential avenue for minimizing sonic boom (ref. 26). The principal observation to be made here relates to the differences in the correlations of theory and experiment found with the near-field and midfield signature results. As noted, the correlation of results at either distance ratio will depend on the characteristics of the near-field signature. Consequently, the near-field signature alone is not a reliable criterion for appraising the relative sonic-boom performance of a given configuration.

Planform effects– With minor exceptions, the degree of planform geometric complexity (tandem, cranked, curved edges, etc.) for the delta, swept, or curved-edge series of wings appears to have little bearing on the accuracy of the predicted signature characteristics for either the near-field or midfield distance conditions. Whereas the theory showed considerable deviation from experiment (as noted previously under lift and Mach number effects), the effects of planform variation (including subsonic, sonic, and supersonic leading edges) were predicted reasonably well. The minor exceptions include models 11 and 12 with curved edges wherein at Mach 1.68 the magnitude of the wing thickness shock (zero lift) showed poor agreement with experiment (see figs. 6(c) and 6(d)). Since both configurations had reasonably smooth area distributions, the discrepancies are a little difficult to explain other than to reiterate the statement that available theory is unsatisfactory for calculating the flow field on low-aspect-ratio wings involving interactions of the three-dimensional tip flow with the two-dimensional flow aft of a supersonic leading edge.

Comparison of Wing Planform Characteristics

Considerable research has been centered for several years on methods of shaping aircraft to reduce sonic-boom overpressure. In the present study, several unconventional wing planforms have been examined to find a favorable shock/expansion interaction characteristic, heretofore undefined by theory, that would provide new insight into techniques for developing improved overpressure signatures in the midfield flight distance range. For discussion, the planforms are grouped into a delta-wing series, a swept-wing series, and a curved-edge-wing series. Conventional planform shapes have been included as base points. Except for the circular wing, the designs of all configurations incorporated nearly a constant wetted area and volume.

Delta-wing series– Increasing the leading-edge sweep angle from 59° to 69° (models 1 and 4) reduced the maximum overpressure about 20 percent at midfield distance ratios for Mach numbers of 1.68 and 2.7 (see figs. 4(a), 4(d), 8(a) and 8(d)). These reductions are attributable to a lengthening of the lift-load distribution on the model. Some of the improvement at the midfield distance for the lower Mach number at $C_L = 0.08$ results from a reduction in the rate of shock coalescence due to a weaker wing shock for the 69° delta wing. Also, note that the combined increase in Mach number and distance ratio advanced the "aging" of the signatures for the higher lift cases to fully developed N-waves and the 10° increase in leading-edge sweep was not sufficient to offset these two "aging" effects.

Two tandem-wing configurations (models 2 and 3) were designed to investigate the effects of lift-induced nose bluntness on the signature characteristics. As discussed by Hicks and Thomas (ref. 26) proper tailoring of nose bluntness, bodyshape, and aft wing position not only can reduce the bow-shock peak pressure compared to conventional sharp-nosed designs, but in addition, can arrest the coalescence of the bow and wing shocks to effect a significant delay in the development of an N-wave. The advantages of nose blunting were first published by Jones (ref. 4) and Carlson (ref. 5). For several years the Ames staff, Ferri (ref. 27), and others have attempted to utilize this blunt-nose concept in the design of low boom aircraft. Models 2 and 3 illustrate two such examples wherein the lift load on the forward wing in combination with the wing and nose volume are intended to generate the required effective bluntness more efficiently in terms of lower wave drag than would result from an equivalent bluntness produced solely by volume. Distributing the lift over two wings also reduces the strength of the rear wing shocks. Both models have total wing areas equal to the wing area of basic model 1 and forward wing areas 1/3 and 1/2, respectively, the basic wing area.

At Mach 1.68, referring first to basic model 1 (fig. 4(a)) at the midfield distance ratio of 130, it was noted previously that the strong wing shock coalesces with the bow shock at C_L between 0.08 and 0.15. In figures 4(b) and 4(c), the redistribution of lift obtained with the tandem wing not only changes the rate of forward advancement of the wing shock with an increase in lift coefficient, but the coalescence of the wing and bow shock can be arrested completely and the wing shock made to retreat toward the tail shock. At Mach 2.7, the effectiveness of the tandem-wing configuration for controlling shock coalescence continues but at a reduced level in comparison to the lower Mach number (see figs. 8(b) and 8(c)). Additional treatment of this shock coalescence phenomenon is given in reference 26. On the basis of the present limited investigation, it is apparent that this design approach involving only the wing geometry can reduce the maximum overpressure of the basic delta wing model by 20 to 40 percent, the amount depending on the design lift coefficient and Mach number.

Swept-wing series– Swept-wing model 5 has the same wetted area and sweep angle of the leading edge as delta-wing model 4 but a somewhat higher aspect ratio and a little less volume. A comparison of the signature characteristics for the two wings (figs. 4(d) and 5(a)) shows that in the near-field the peak wing overpressure of the swept-wing is about 30 percent less than that of the delta wing; however, at the midfield distance ratio of 130, the difference is about 10 percent. Also, the signature development with an increase in lift coefficient for the two wings is very similar at Mach 1.68. At Mach 2.7, the overpressure characteristics of the swept wing and 69° delta wing models are very similar (figs. 8(d) and 9). Hence, in this example, the lengthening of the lift loading

provided by the swept wing is more than offset by the lower aspect ratio of the delta wing. At an intermediate test Mach number of 2 (fig. 7), the swept wing does not show any large adverse effects of increased Mach number. The maximum overpressure characteristics remain constant at the midfield distance and only the impulse shows an increase in comparison to the Mach 1.68 results.

Tests of a swept-forward wing (model 6, fig. 5(b)) indicate no unusual shock interaction characteristics since the pressure signatures at $C_L = 0.15$ were predicted surprisingly well at both the near-field and midfield distances. Tests of M and W wings (models 7 and 8, respectively) extend the shock interaction study still further to examine the potential effectiveness of cranked leading edges for reducing the strength of the wing leading-edge shock. In figures 5(c) and 5(d), the data show no improvement in overpressure characteristics from either of the two cranked leading-edge wings. In comparison to the base swept wing (model 5), the M and W wings generally increased the shock overpressures by as much as 20 percent and this effect was predicted reasonably well by theory.

Curved-edge wing series– Another method investigated for reducing the strength of the wing-shock system involved curvature of the wing leading edges. With a trapezoidal wing (model 9) as a base, three wings were tested at Mach 1.68 including a straked (model 10), ogee (model 11), and circular (model 12) planform (figs. 6(a)–6(d)). As expected, the base trapezoidal wing, with an abrupt change in cross-sectional area distribution, had the highest overpressure characteristics of any of the wings of this investigation (fig. 10). The addition of curved strakes (model 10) to the trapezoidal wing did little to weaken the wing shock. Likewise, the addition of curvature at the wing tips illustrated with the ogee planform model 11 was relatively ineffective. The similarity of the results for models 10 and 11 with those for the straight leading-edge delta-wing model 1 is easily seen. Thus, local changes in shape of the wing planform appear to have little overall effect on the shock-system development. The average sweep angle of the leading edge is clearly one of the dominant wing geometric parameters in the control of the maximum overpressure characteristics. Eliminating all straight edges on both the leading and trailing edges by means of a circular wing (model 12) does not significantly reduce sonic-boom overpressure. This configuration, having the lowest geometric aspect ratio of any of the wings tested, required somewhat higher angles of attack to reach the test lift coefficient. The higher attitude of the model and the unswept maximum thickness ridge line of the wing are possible factors in the poor overpressure characteristics for this configuration.

Configuration Design for Low Boom

A brief summary of the experimental maximum overpressures for the wing shock (where identifiable as for a near-field signature or as the combined bow/wing shock as for an N-wave) of the various models tested is presented in figure 10 for the near-field (wind tunnel) and midfield (flight) distance ratios at Mach numbers 1.68 and 2.7. A comparison of the results at the two distance ratios and Mach numbers reveals some definite changes in the relative magnitudes of the maximum overpressures. Consequently, to attain a certain minimum overpressure will require point designs oriented fairly specifically to the flight lift coefficient, altitude, and Mach number of the mission. While emphasis here has been centered primarily on the wing/bow shock for the purpose of gaining additional insight into the shock interaction and coalescence characteristics for a range of wing planforms, an equal concern is needed for the tail shock region which was not entirely possible with the present experimental limitations. Future investigations will require the development of special experimental methods or techniques if valid tail-shock characteristics are to be studied.

Configuration design for low boom based on current technology appears to be following either of two options: (1) adherence to conventional structural design criteria that lead to configuration lengths where shocks are unavoidable, or (2) relaxation of structural design criteria that can lead to extreme configuration lengths to provide for overpressure rise times of sufficient duration to avoid shocks entirely. The design objective in the former case consists in shaping the vehicle for maximum attenuation of overpressure jumps and/or minimum coalescence of shocks while, in the latter case, the design objective consists in shaping the vehicle to obtain only isentropic compressions for minimum length and maximum volume. Option 1 involves maximum structural efficiency and maximum volume and is reached through effective blunting of the forebody area distribution and lengthening of the lift distribution (which may lead to high wave drag and high drag due to lift). Option 2 entails a minimum structural efficiency and minimum volume and will require significant advances in the technology of structures. Hence, optimization of aircraft design for low sonic boom considerations for either option is not consistent with design features that historically have been synonymous with optimization of aircraft for maximum aerodynamic efficiency and/or performance. Or, stated another way, optimization of the aerodynamic efficiency of a given vehicle is neither a guarantee nor a valid criterion for low boom despite a popularly held conception to the contrary.

CONCLUDING REMARKS

A wind-tunnel and analytical investigation has been conducted to assess the overpressure characteristics of a series of wing planforms mounted on a body of revolution at Mach numbers of 1.7, 2.0, and 2.7. The wings included both conventional and unconventional planforms.

Agreement of sonic-boom theory with experiment was found to depend generally on configuration slenderness (as controlled by geometry, lift, Mach number, load distribution, etc.), the type of signature, and the distance ratio.

The degree of complexity of wing planform shape appears to have little bearing on the accuracy with which the signature characteristics were predicted for either the very near-field or midfield distance ratios.

Because of the nonlinear distortions that occur in the propagation of a waveform in the atmosphere, direct comparisons of very near-field signatures are not a valid guide to the relative level of overpressure performance for a given configuration at midfield distances.

Wing planform design can significantly reduce the magnitude of shock overpressures at midfield distances by about 20 to 40 percent in comparison with the overpressures for comparable conventional wing planforms.

Local changes in wing leading-edge shape obtained with strakes, cranks, or curvature were relatively ineffective in altering the overpressure characteristics of the basic planform.

Supersonic aircraft designed for low sonic-boom at a specific Mach number will not have broad application over the full supersonic Mach number range nor will such designs be in consonance with design features that produce maximum aerodynamic efficiency and performance.

Ames Research Center
National Aeronautics and Space Administration
Moffett Field, Calif., 94035, September 14, 1972

REFERENCES

1. Seebass, A. R., Ed.: Sonic Boom Research. NASA SP–147, 1967.

2. Schwartz, Ira R., Ed.: Second Conference on Sonic Boom Research. NASA SP–180, 1968.

3. Schwartz, Ira R., Ed.: Third Conference on Sonic Boom Research. NASA SP–255, 1971.

4. Jones, L. B.: Lower Bounds for Sonic Bangs. Journal R.A.S., vol. 65, no. 606, June 1961, pp. 433–436.

5. Carlson, Harry W.: The Lower Bound of Attainable Sonic-Boom Overpressure and Design Methods of Approaching This Limit. NASA TN D–1494, 1962.

6. Carlson, Harry W.; Mack, Robert J.; and Morris, Odell A.: A Wind Tunnel Investigation of the Effect of Body Shape on Sonic Boom Pressure Distributions. NASA TN D–3106, 1965.

7. McLean, F. Edward: Some Nonasymptotic Effects on the Sonic Boom of Large Airplanes. NASA TN D–2877, 1965.

8. Hague, D. S.; and Jones, R. T.: Application of Multivariable Search Techniques to the Design of Low Sonic Boom Overpressure Body Shapes. NASA SP–255, 1970, pp. 307–323.

9. Hayes, Wallace D.: Linearized Supersonic Flow. Rept. A1–222, North American Aviation, Inc., June 1947.

10. Jones, Robert T.: Theory of Wing-Body Drag at Supersonic Speeds. NACA RM A53H18a, 1953.

11. Lomax, Harvard: The Wave Drag of Arbitrary Configurations in Linearized Flows as Determined by Areas and Forces in Oblique Planes. NACA RM A55A18, 1955.

12. Whitham, G. B.: The Flow Pattern of a Supersonic Projectile. Commun. Pure Appl. Math., vol. V, no. 3, Aug. 1952, pp. 301–348.

13. Carmichael, Ralph L.; Castellano, Charles R.; and Chen, Chuan F.: The Use of Finite Element Methods for Predicting the Aerodynamics of Wing-Body Combinations. Analytic Methods in Aircraft Aerodynamics. NASA SP–228, 1970, pp. 37–51.

14. Carlson, Harry W.: An Investigation of the Influence of Lift on Sonic Boom Intensity by Means of Wind-Tunnel Measurements of the Pressure Fields of Several Wing-Body Combinations at Mach Numbers of 2.01. NASA TN D–881, 1961.

15. Carlson, Harry W.: Correlation of Sonic Boom Theory With Wind-Tunnel and Flight Measurements. NASA TR R–213, Dec. 1964.

16. Morris, Odell A.; Lamb, Milton; and Carlson, Harry W.: Sonic-Boom Characteristics in the Extreme Near Field of a Complex Airplane Model at Mach Numbers 1.5, 1.8 and 2.5. NASA TN D–5755, 1970.

17. Harris, Roy V., Jr.: An Analysis and Correlation of Aircraft Wave Drag. NASA TM X–947, 1964.

18. Woodward, Frank A.: Pressure Signature Estimation at High Mach Numbers. NASA SP–255, 1971, pp. 437–441.

19. Kutler, Paul; and Lomax, Harvard: Shock-Capturing, Finite-Difference Approach to Supersonic Flows. Journal of Spacecraft and Rockets, vol. 8, no. 12, Dec. 1971, pp. 1175–1182.

20. Hicks, Raymond M.; and Mendoza, Joel P.: Prediction of Aircraft Sonic Boom Characteristics From Experimental Near Field Results. NASA TM X–1477, 1967.

21. Mendoza, Joel P.; and Hicks, Raymond M.: Further Studies of the Extrapolation of Near-Field Overpressure Data. NASA TM X–2219, 1971.

22. Mendoza, Joel P.; and Hicks, Raymond M.: On the Extrapolation of Measured Near-Field Pressure Signatures of Unconventional Configurations. NASA SP–255, 1971, pp. 385–392.

23. Thomas, Charles L.: Extrapolation of Wind-Tunnel Sonic Boom Signatures Without Use of a Whitham F–Function. NASA SP–255, 1971, pp. 205–217.

24. Carlson, Harry W.; McLean, F. Edward; and Shrout, Barrett L.: A Wind-Tunnel Study of Sonic-Boom Characteristics for Basic and Modified Models of a Supersonic Transport Configuration. NASA TM X–1236, 1966.

25. Hayes, W. D.; Haefeli, R. C.; and Kulsrud, H. E.: Sonic Boom Propagation in a Stratified Atmosphere, With Computer Program. NASA CR–1299, 1969.

26. Hicks, Raymond M.; and Thomas, Charles L.: A Preliminary Report on Shock Coalescence. NASA SP–255, 1970, pp. 297–305.

27. Ferri, Antonio; and Ismail, Ahmed: Report on Sonic Boom Studies. Part I–Analysis of Configurations. NASA SP–180, 1968, pp. 73–88.

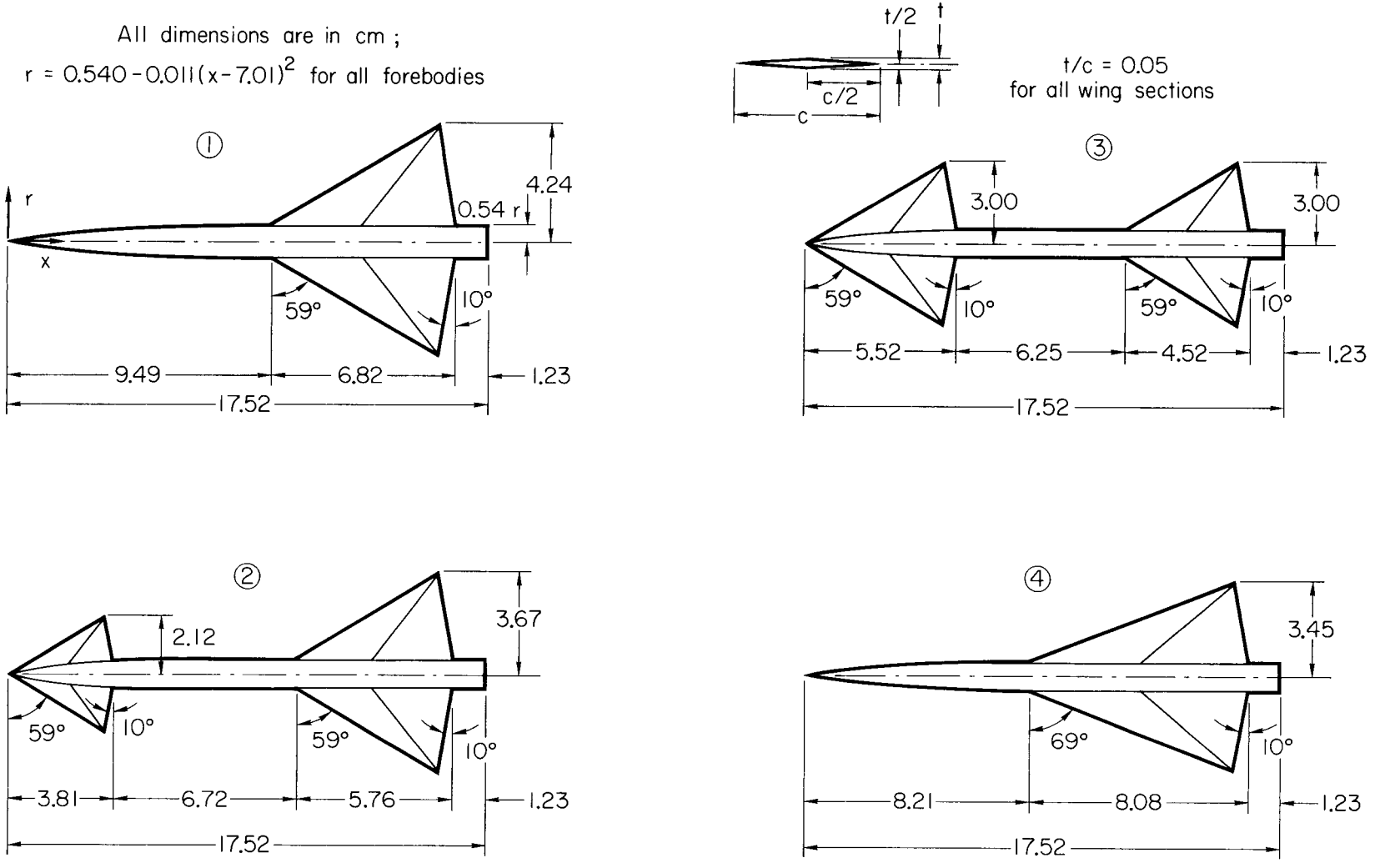

(a) Delta-wing series.

Figure 1.– Dimensions of the test configurations.

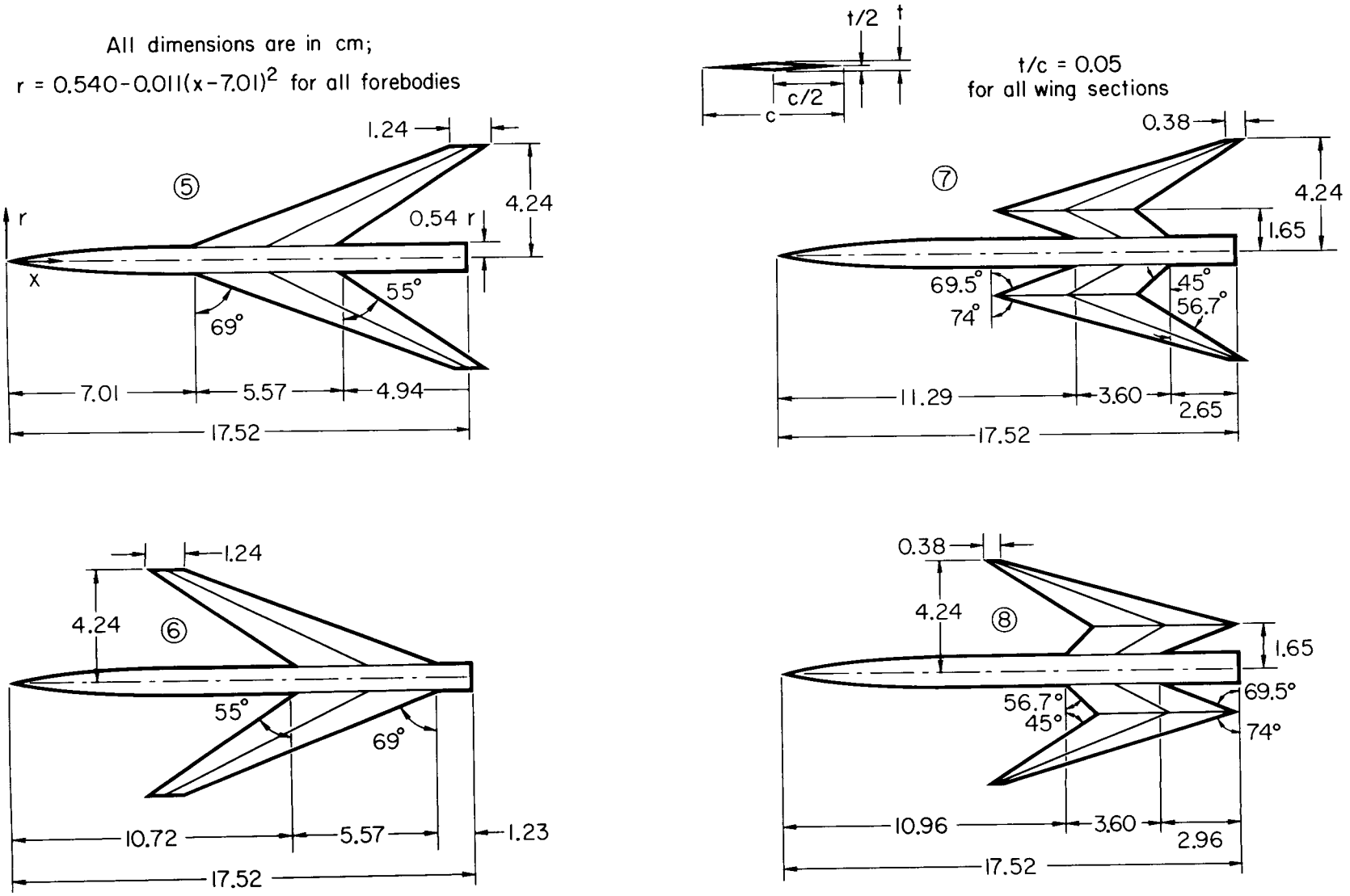

(b) Swept-wing series.

Figure 1.– Continued.

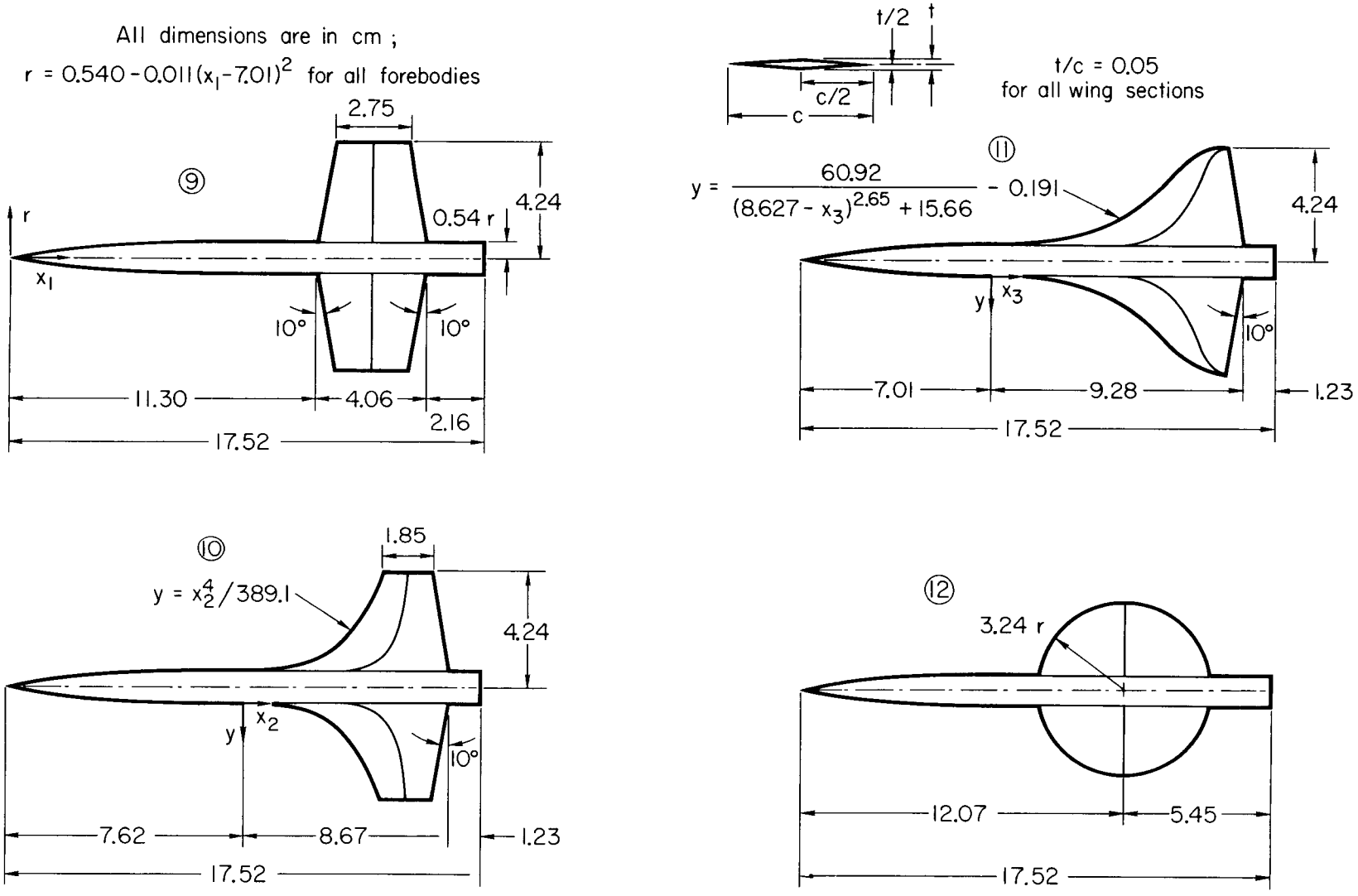

(c) Curved-edge wing series.

Figure 1.– Concluded.

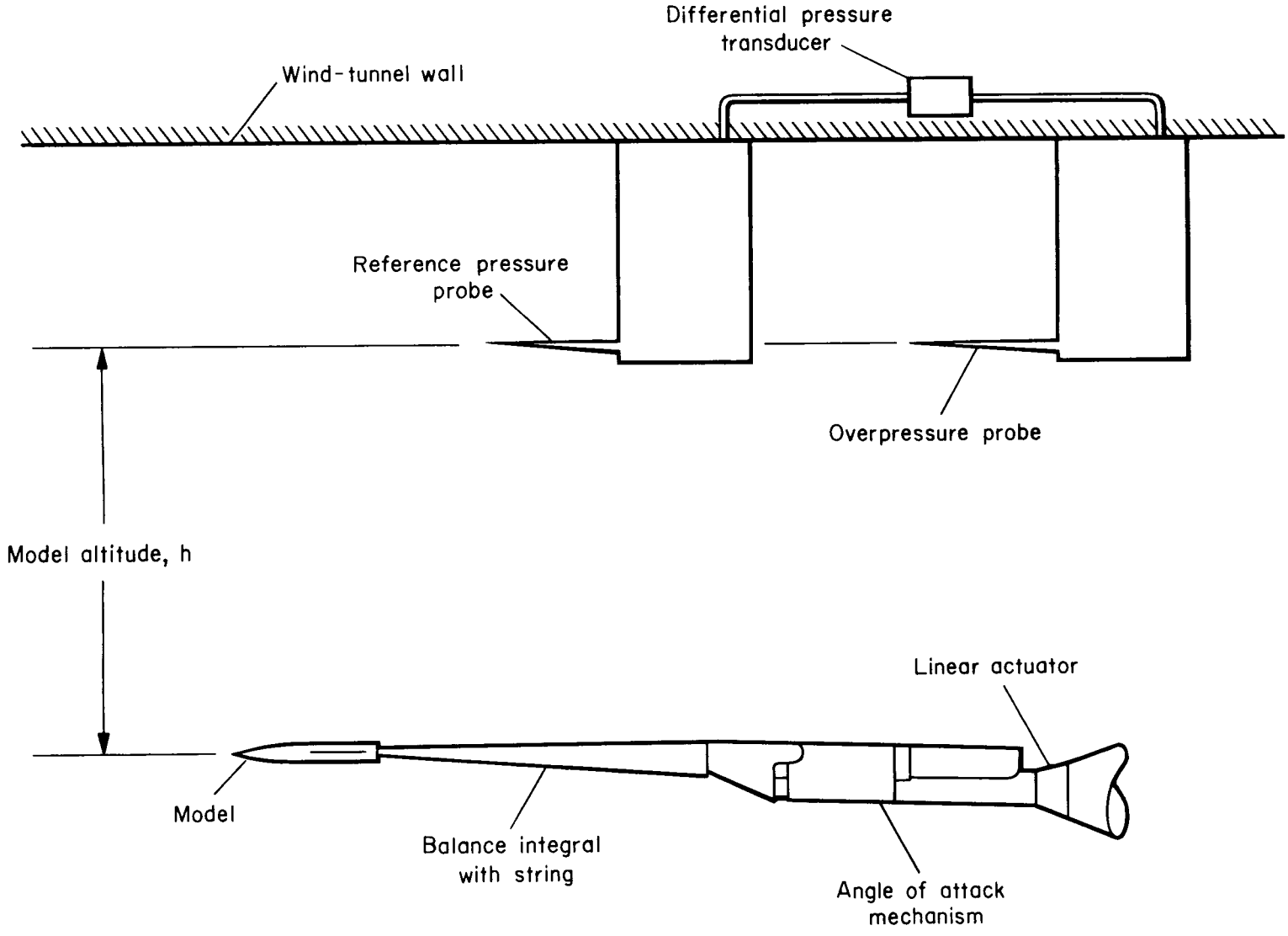

Figure 2.– Wind-tunnel apparatus.

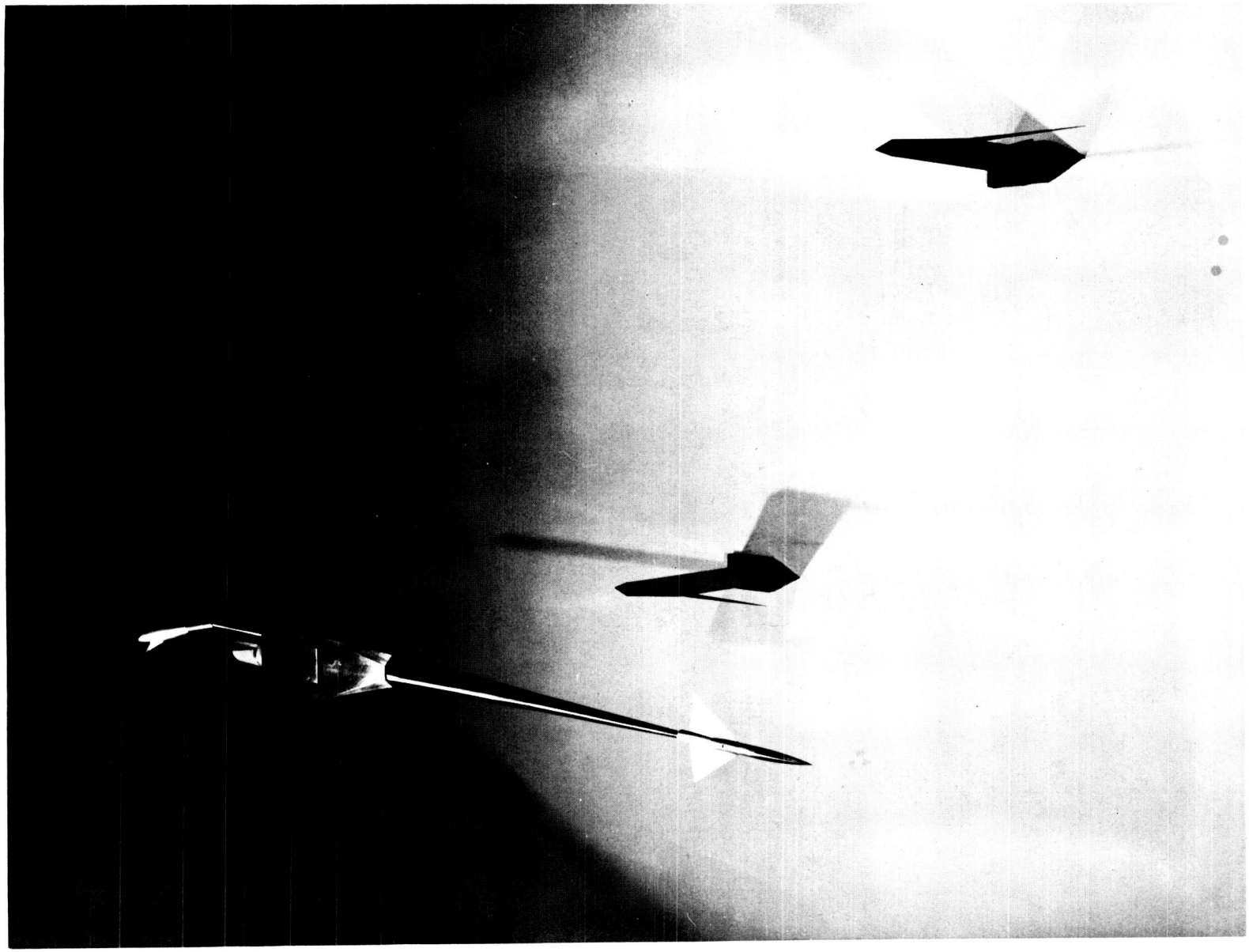

Figure 3.– Test installation.

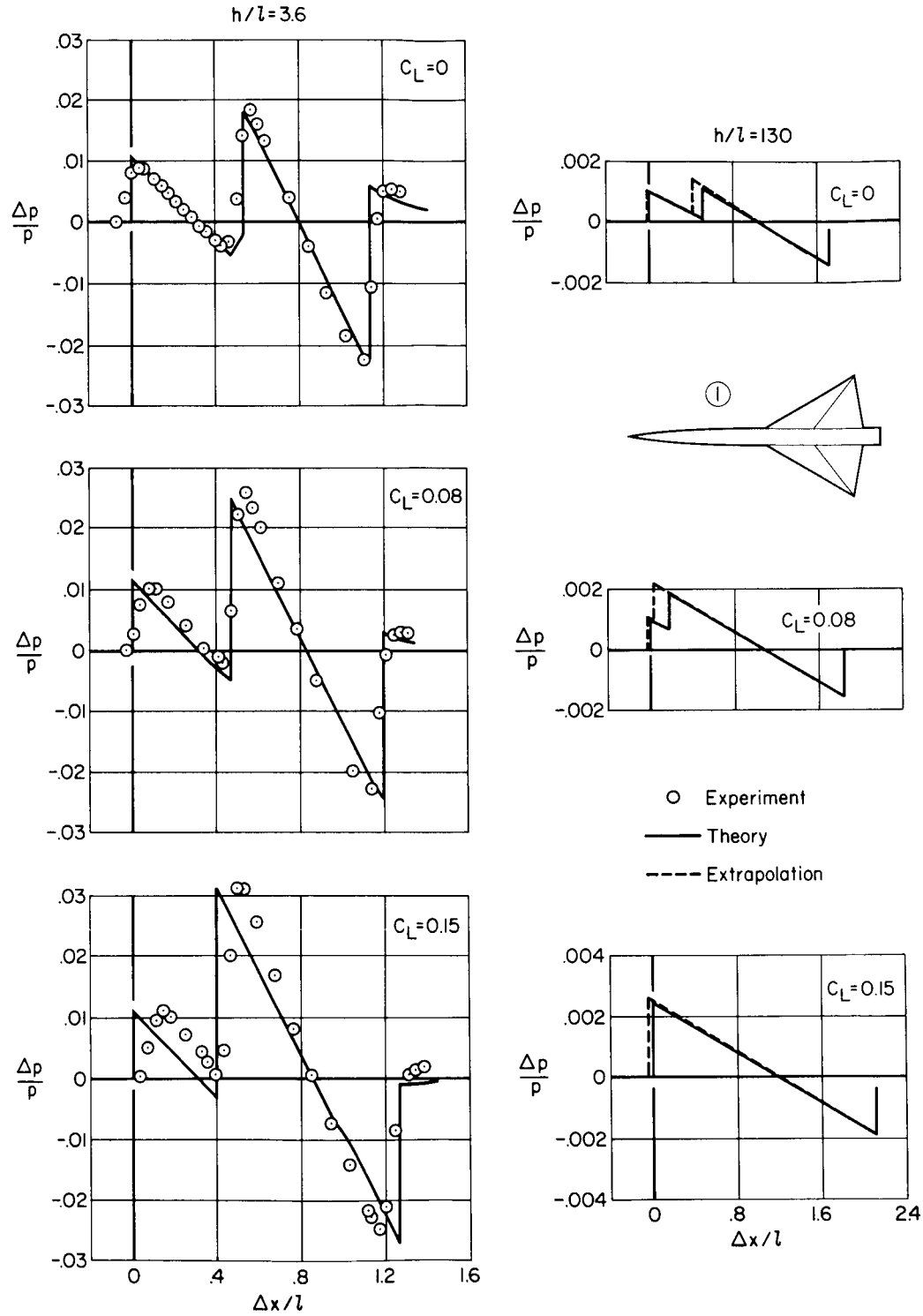

(a) Model 1.

Figure 4.– Comparison of experimental and theoretical pressure signatures; delta-wing series, M = 1.68.

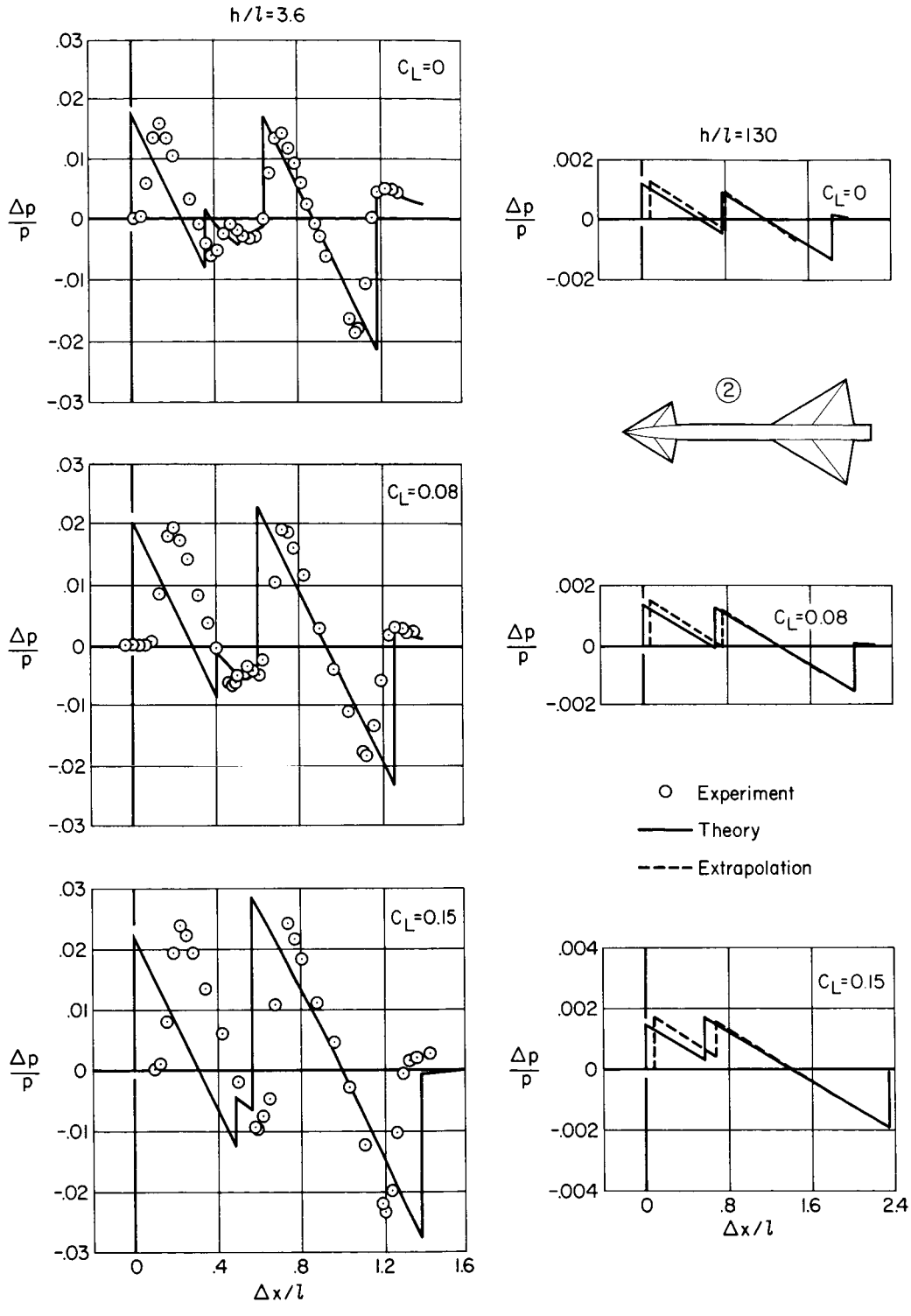

(b) Model 2.

Figure 4.– Continued.

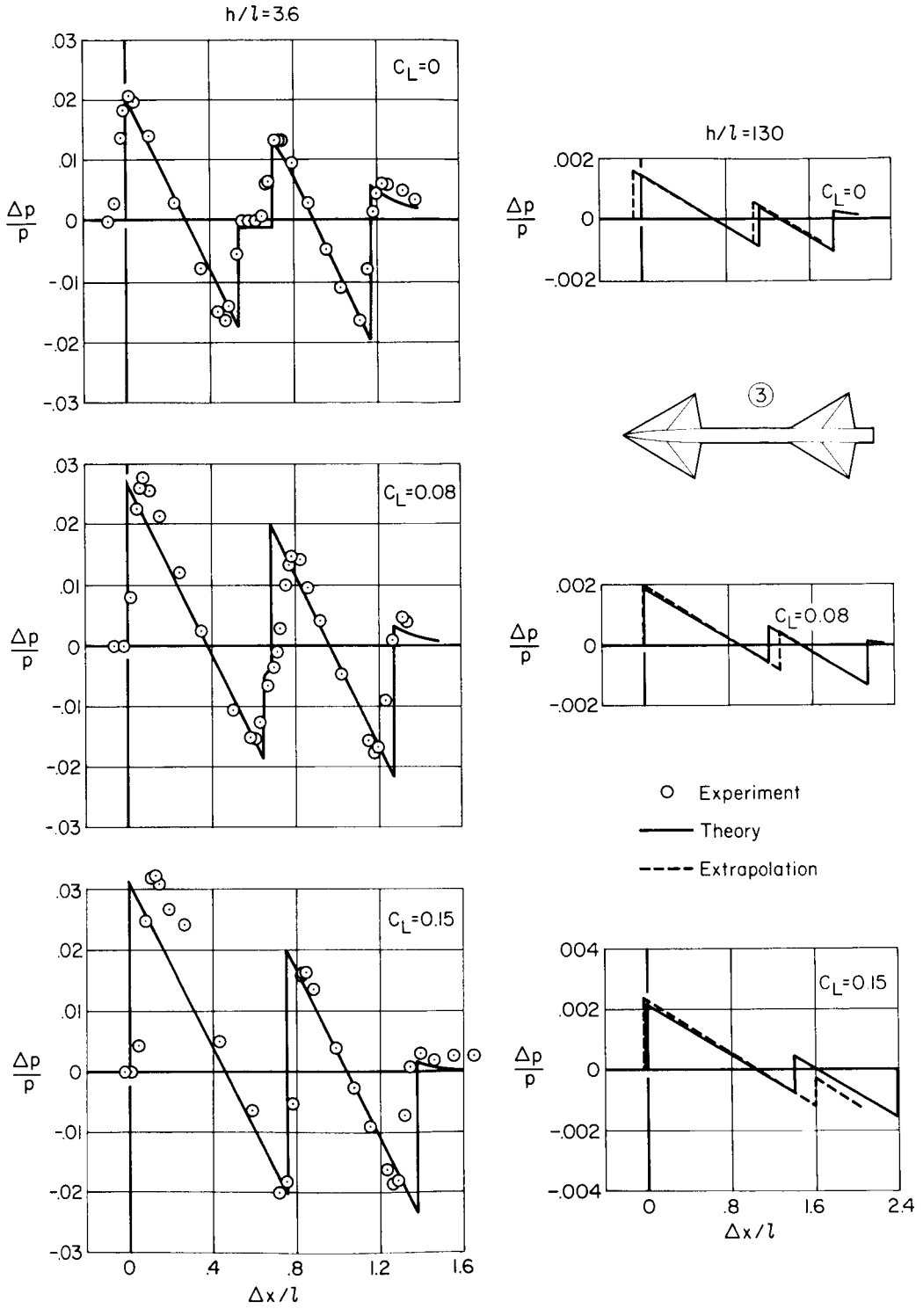

(c) Model 3.

Figure 4.– Continued.

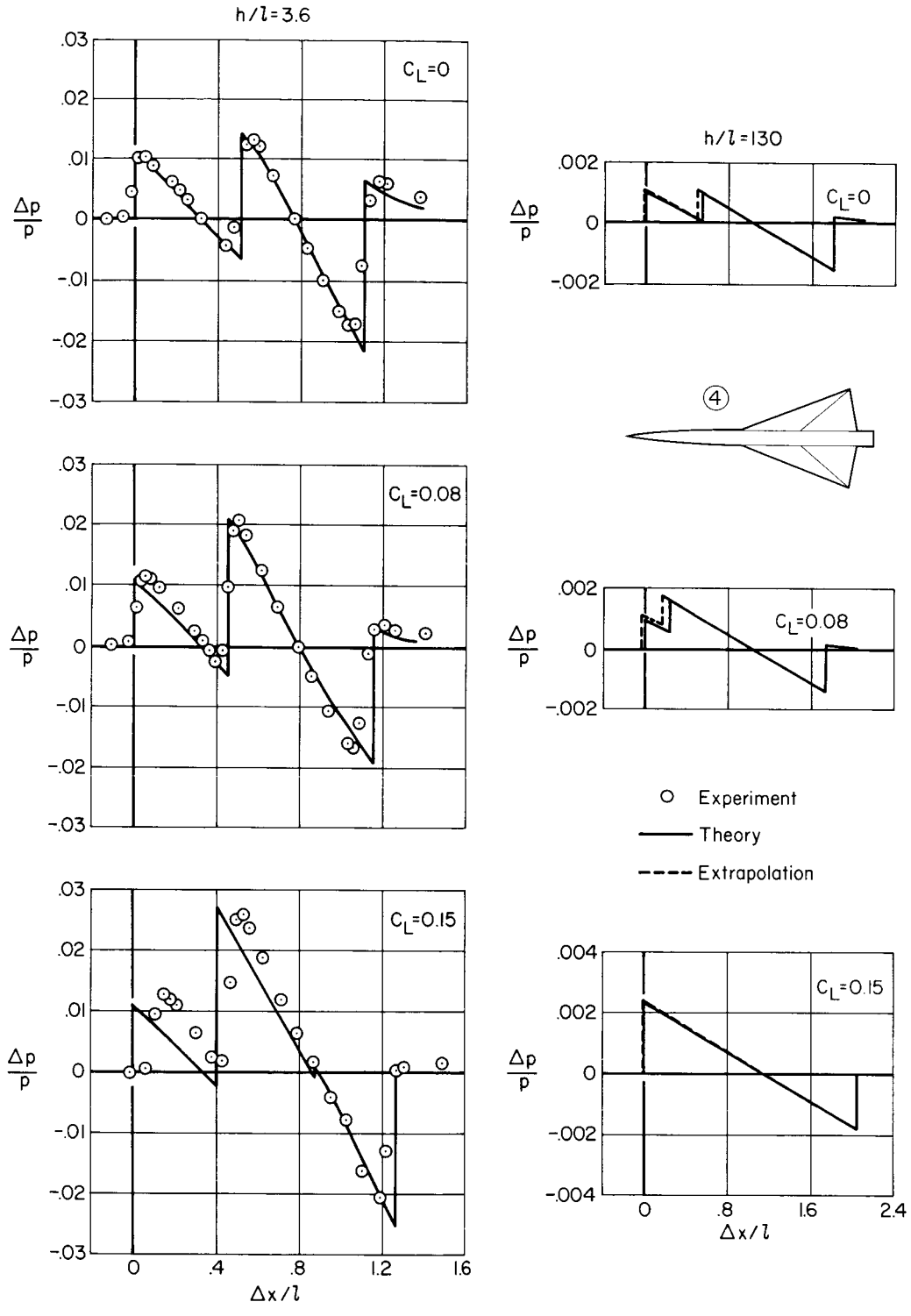

(d) Model 4.

Figure 4.– Concluded.

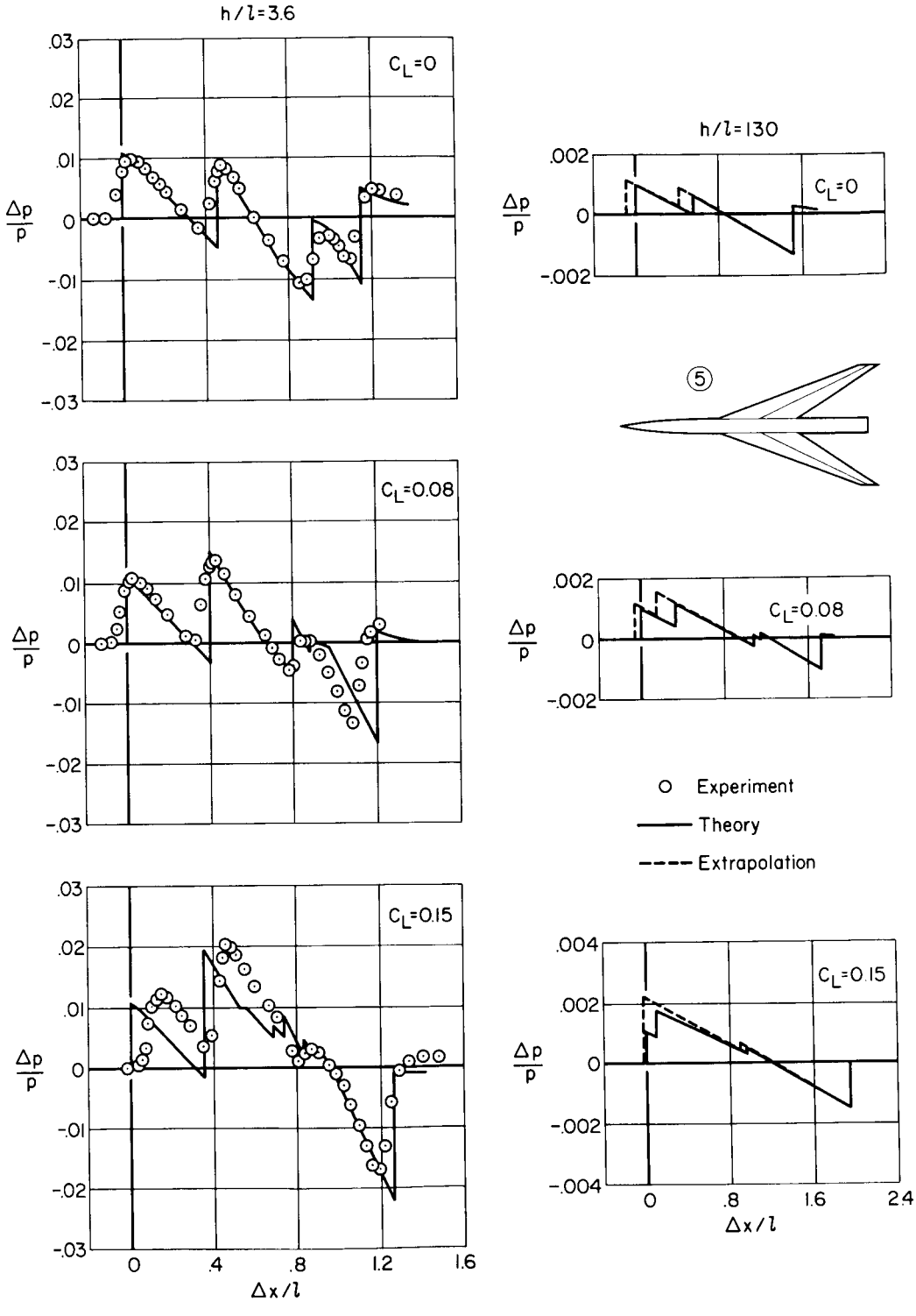

(a) Model 5.

Figure 5.– Comparison of experimental and theoretical pressure signatures; swept-wing series, M = 1.68.

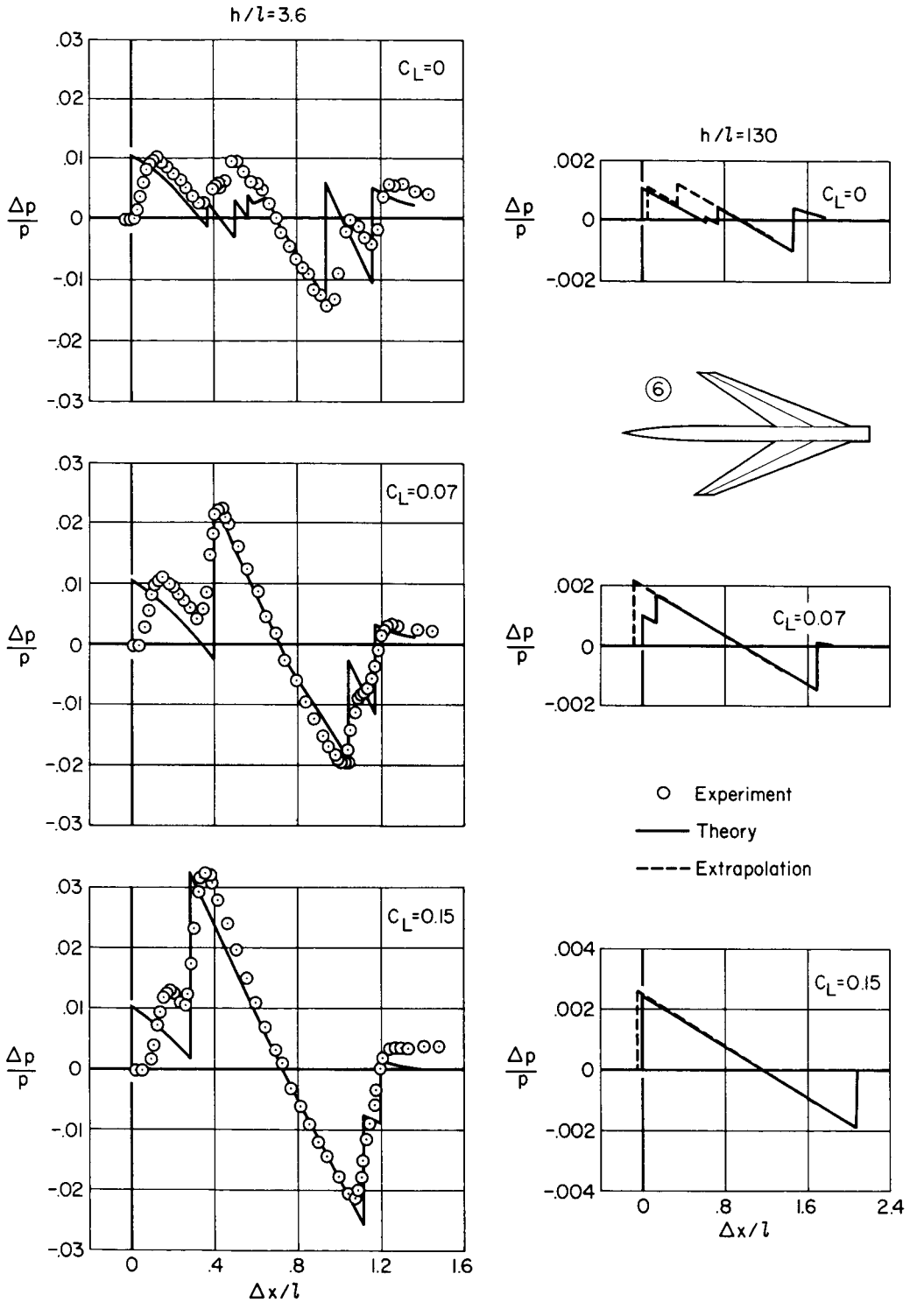

(b) Model 6.

Figure 5.– Continued.

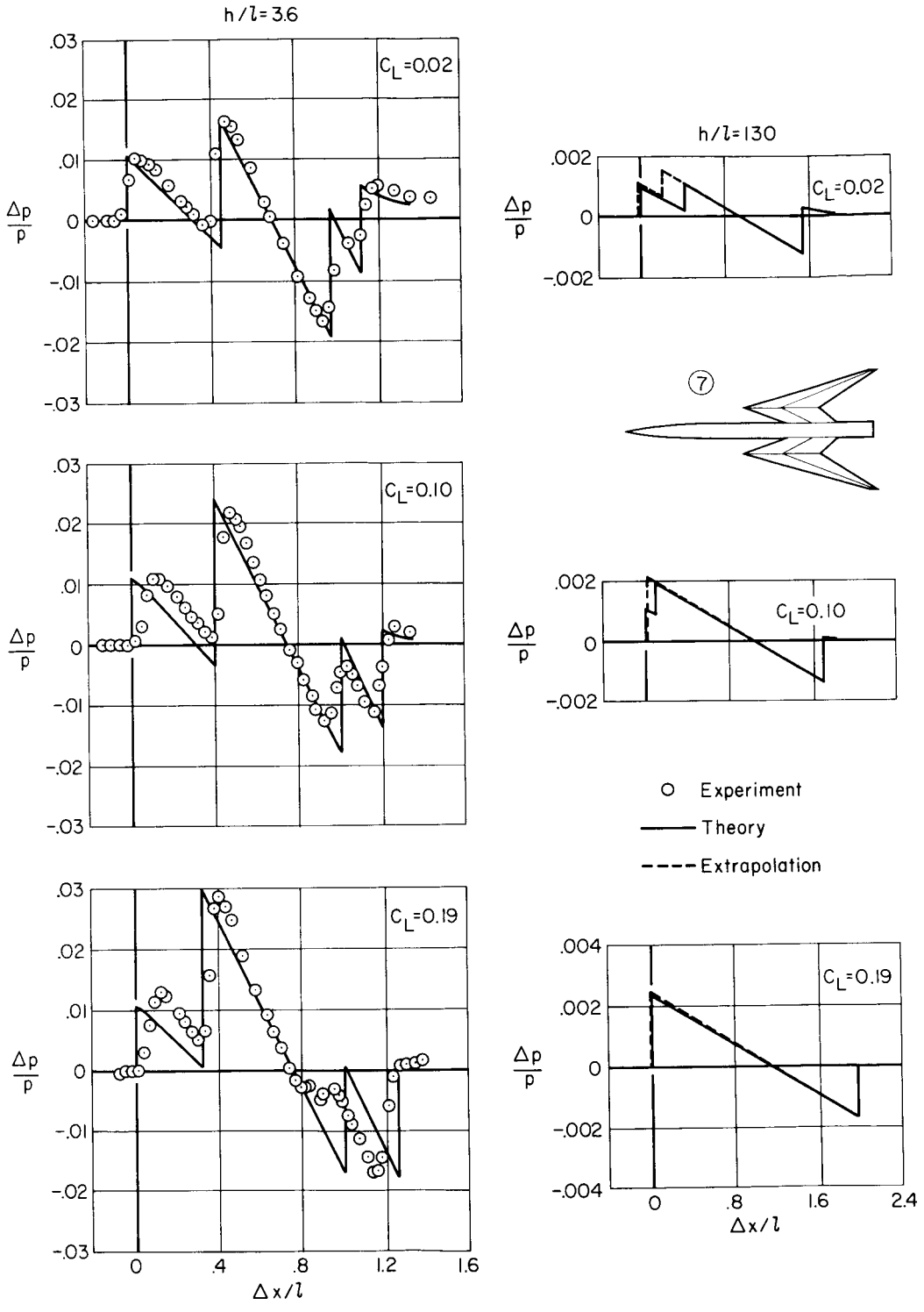

(c) Model 7.

Figure 5.– Continued.

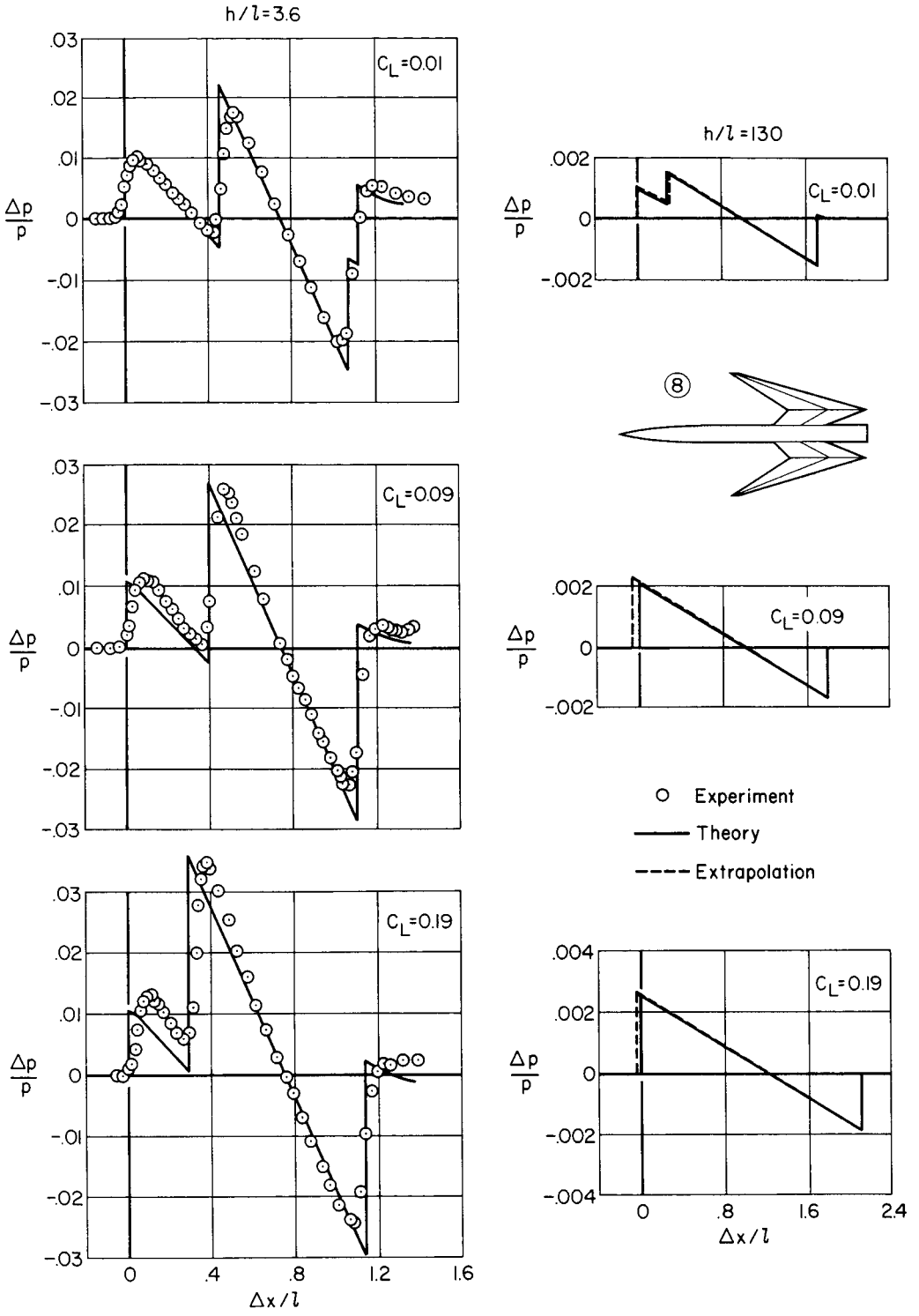

(d) Model 8.

Figure 5.– Concluded.

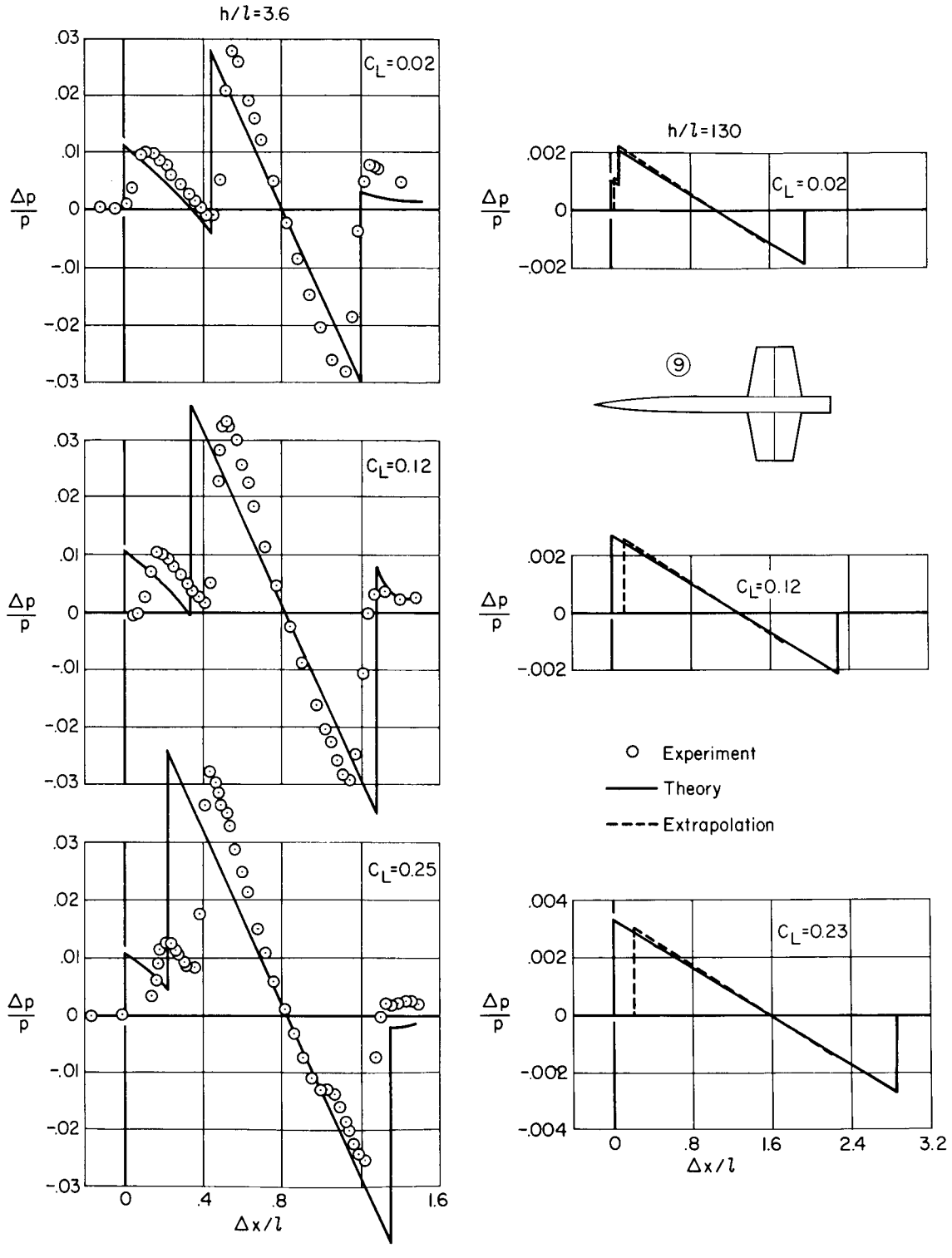

(a) Model 9.

Figure 6.– Comparison of experimental and theoretical pressure signatures; curved-edge series, M = 1.68.

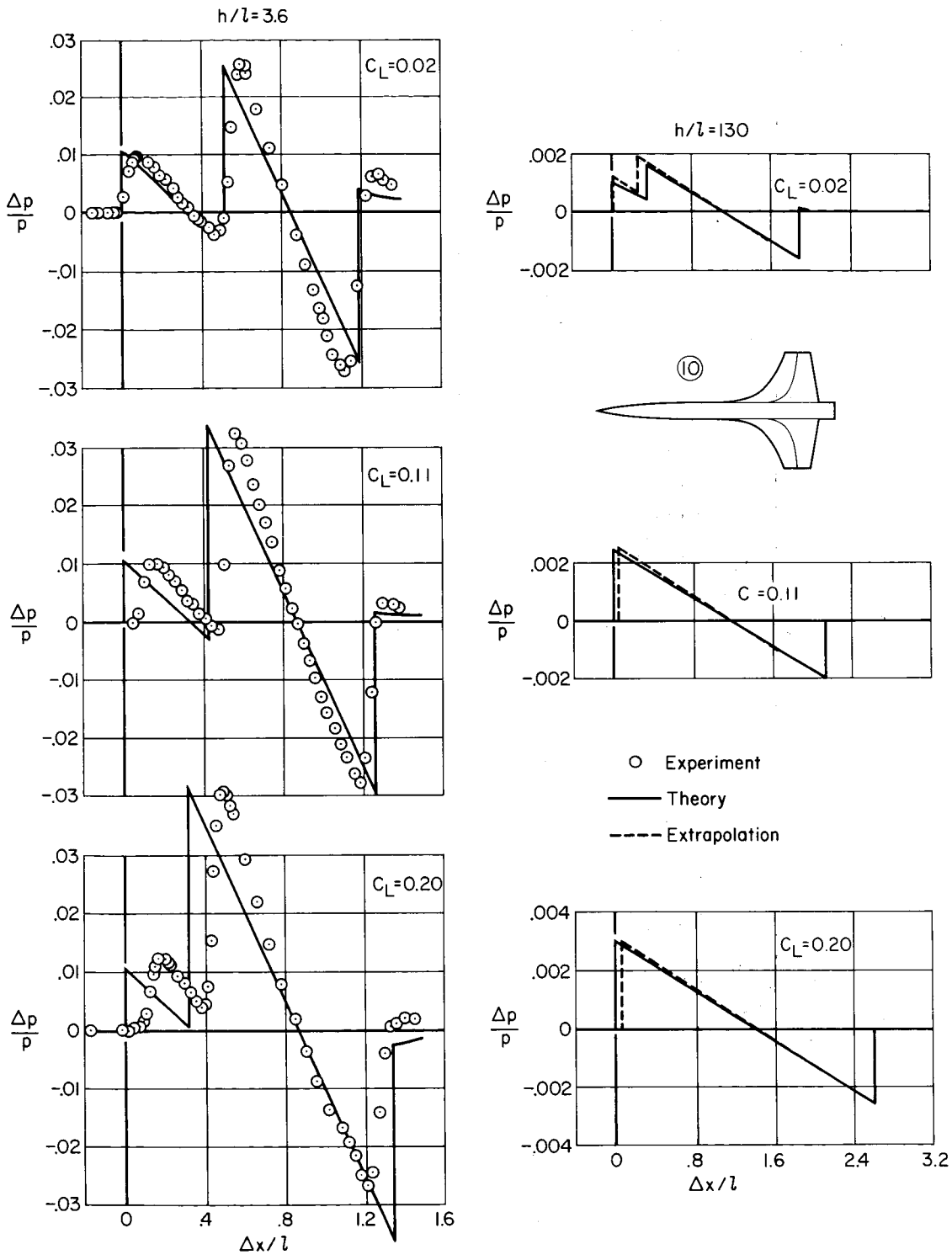

(b) Model 10.

Figure 6.– Continued.

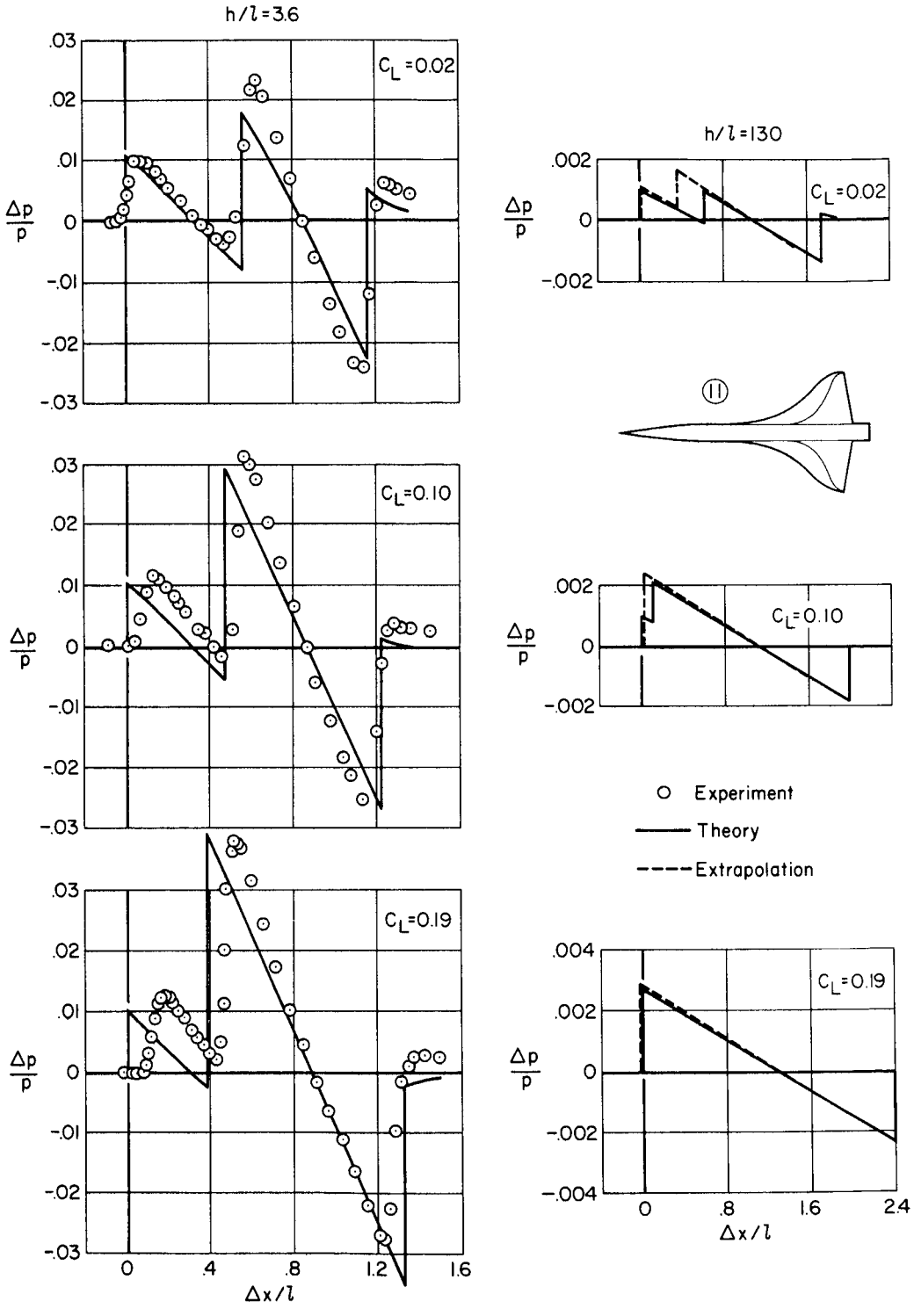

(c) Model 11.

Figure 6.– Continued.

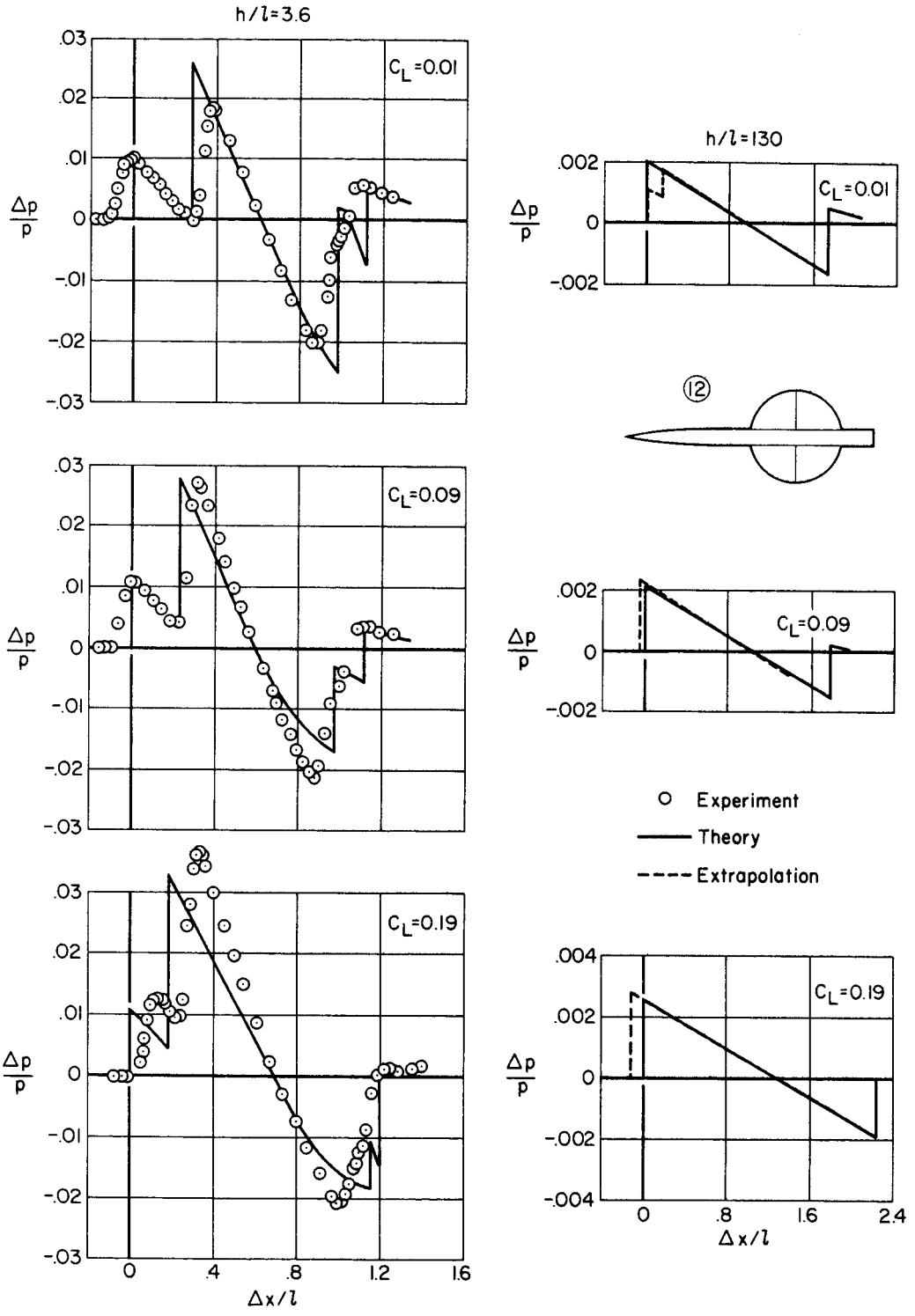

(d) Model 12.

Figure 6.– Concluded.

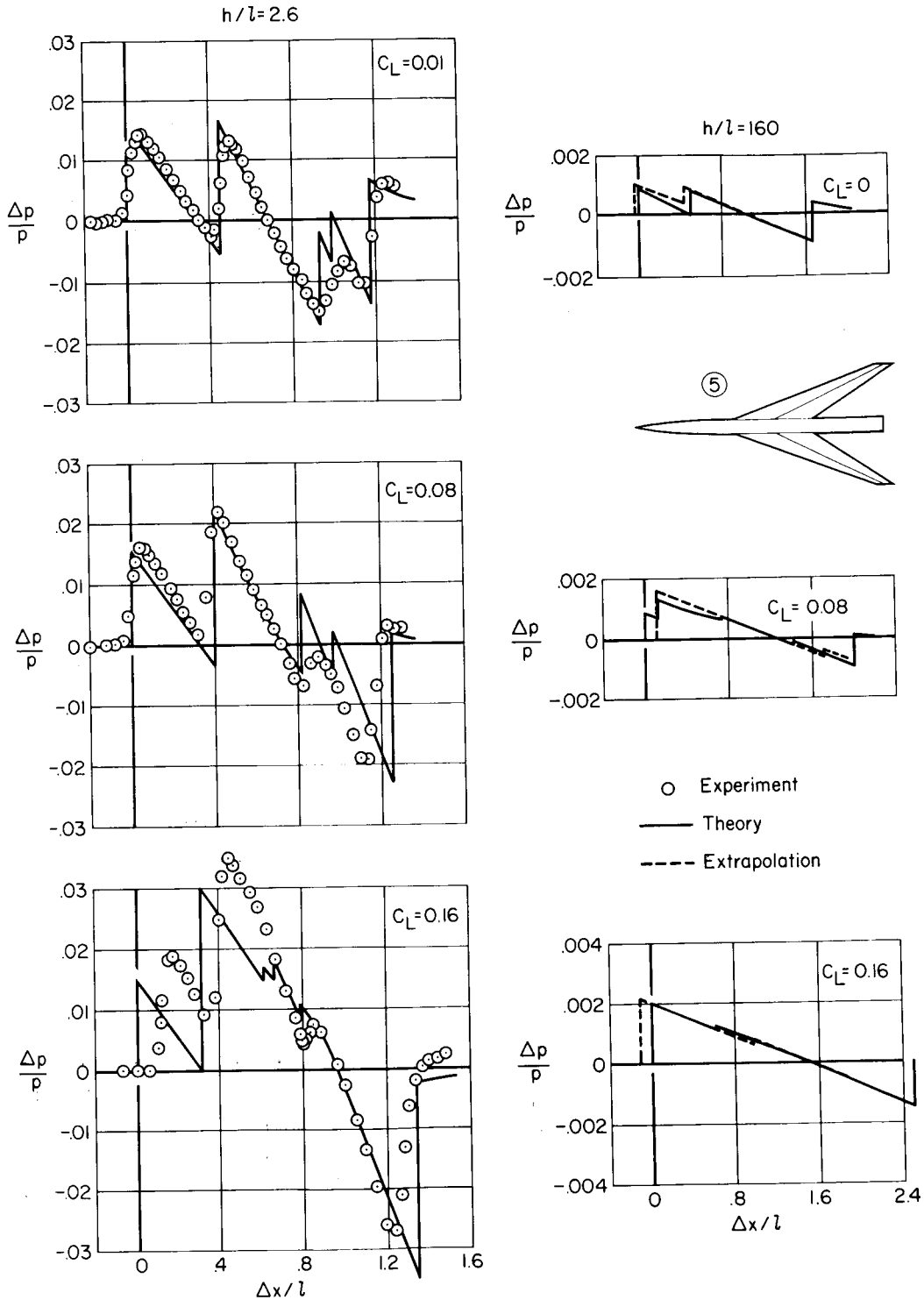

Figure 7.– Comparison of experimental and theoretical pressure signatures for model 5; M = 2.0.

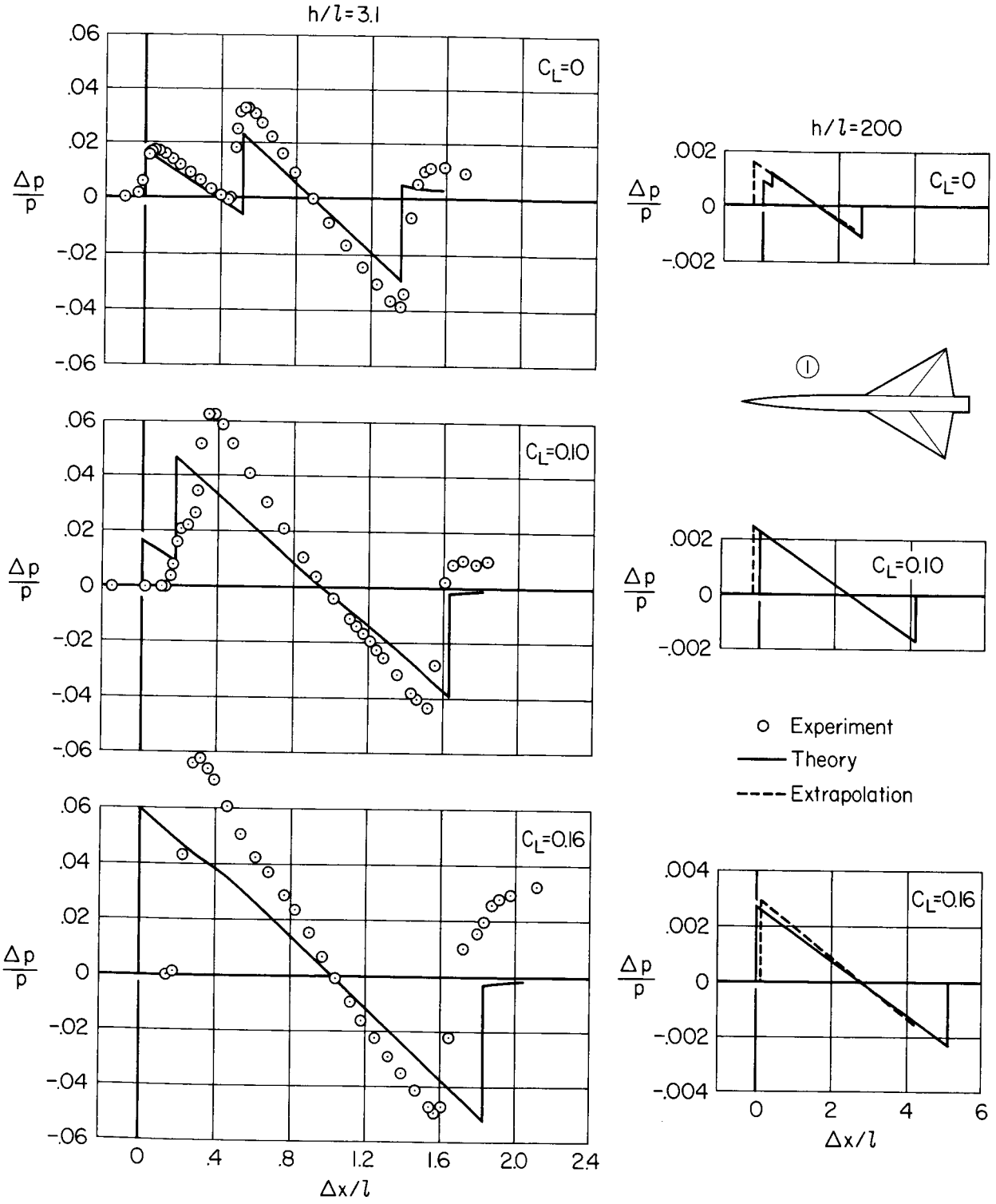

(a) Model 1.

Figure 8.– Comparison of experimental and theoretical pressure signatures; delta-wing series, M = 2.70.

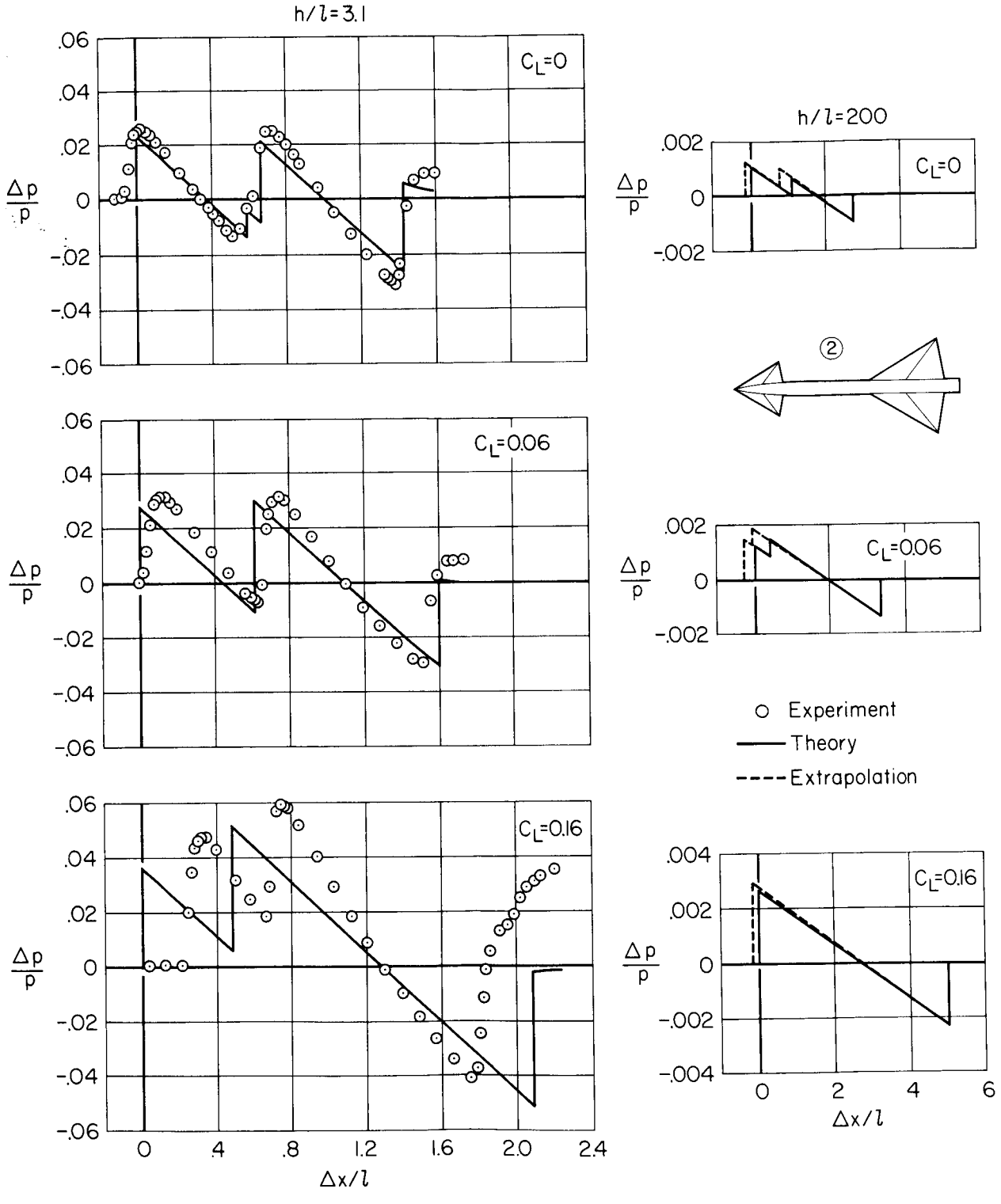

(b) Model 2.

Figure 8.– Continued.

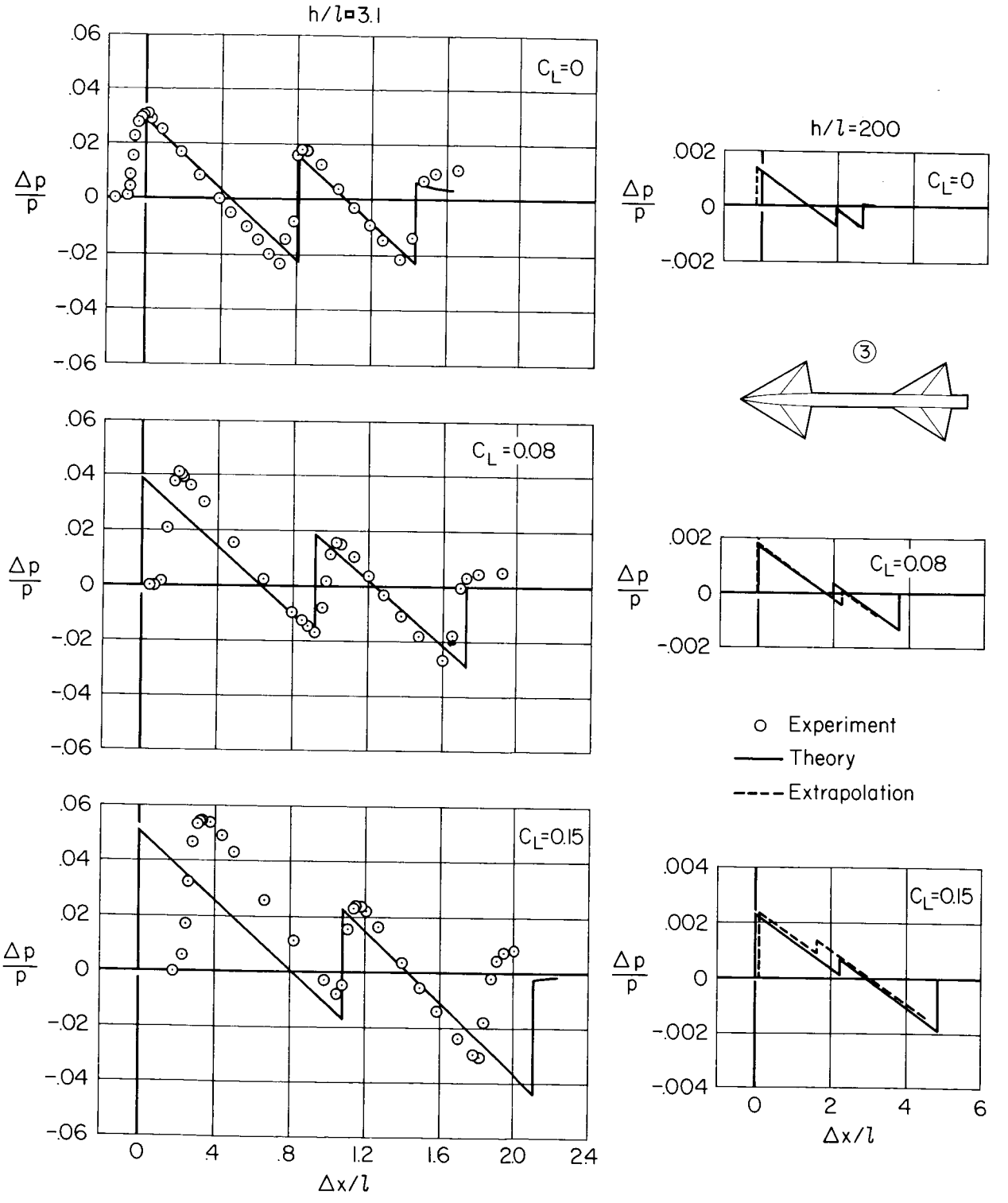

(c) Model 3.

Figure 8.– Continued.

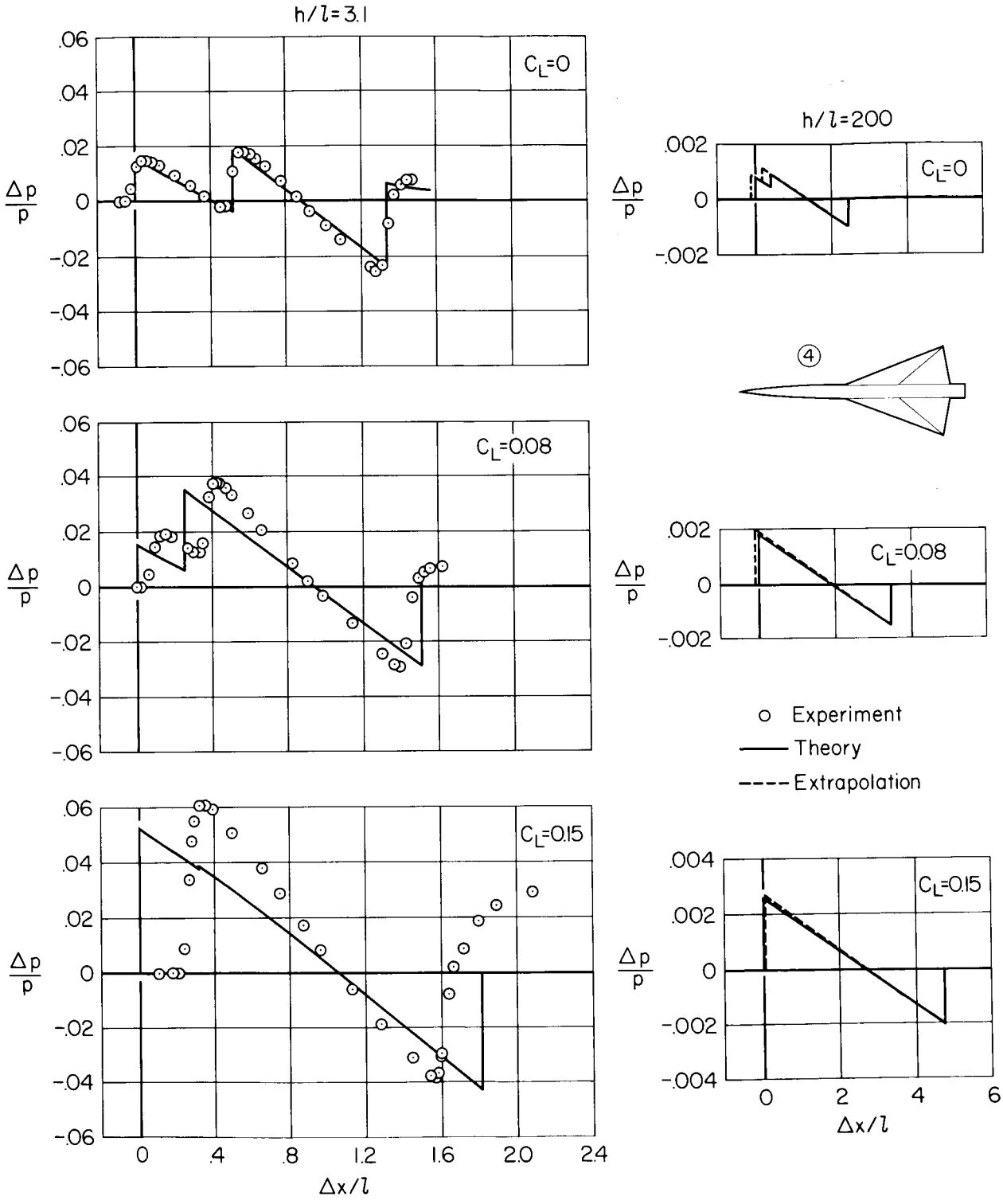

(d) Model 4.

Figure 8.– Concluded.

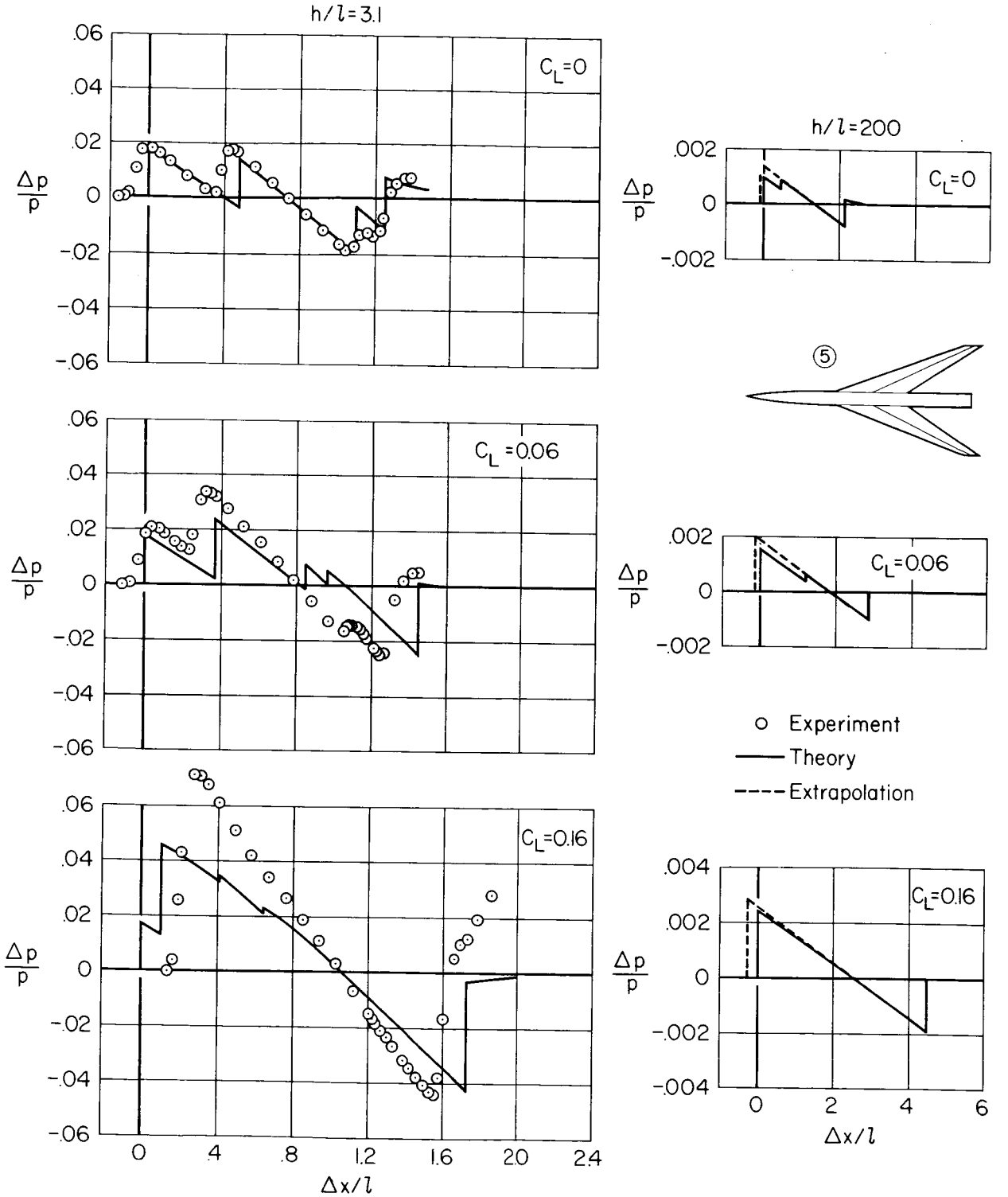

Figure 9.– Comparison of experimental and theoretical pressure signatures for model 5; M = 2.70.

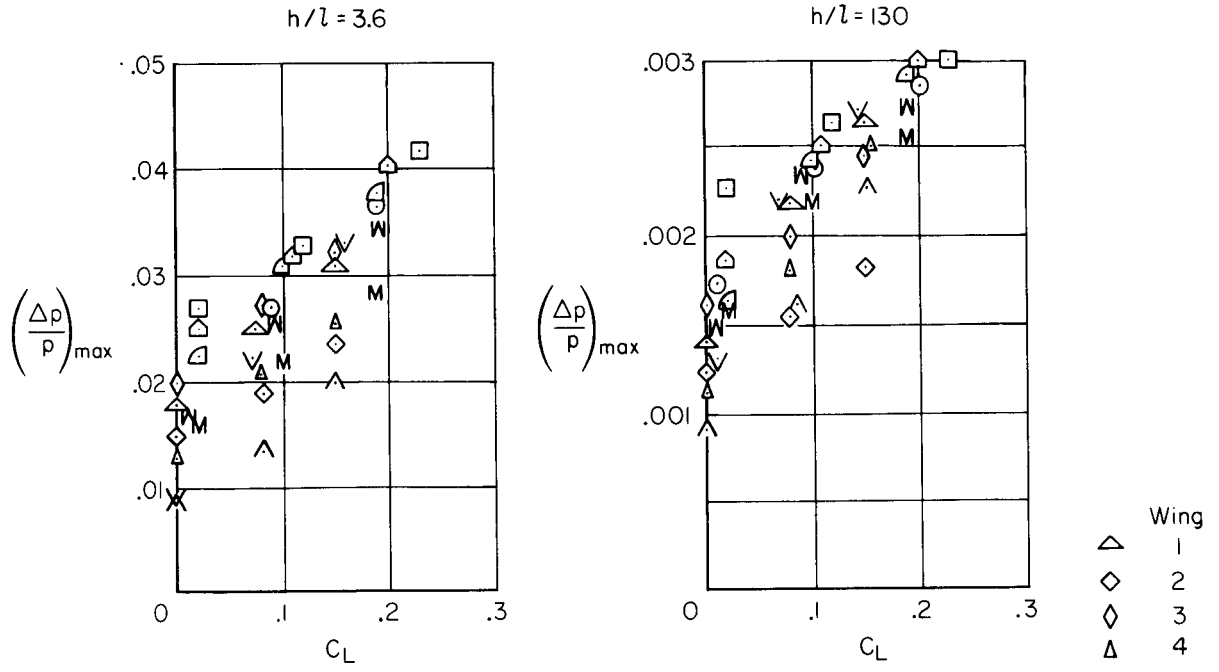

(a) M = 1.68

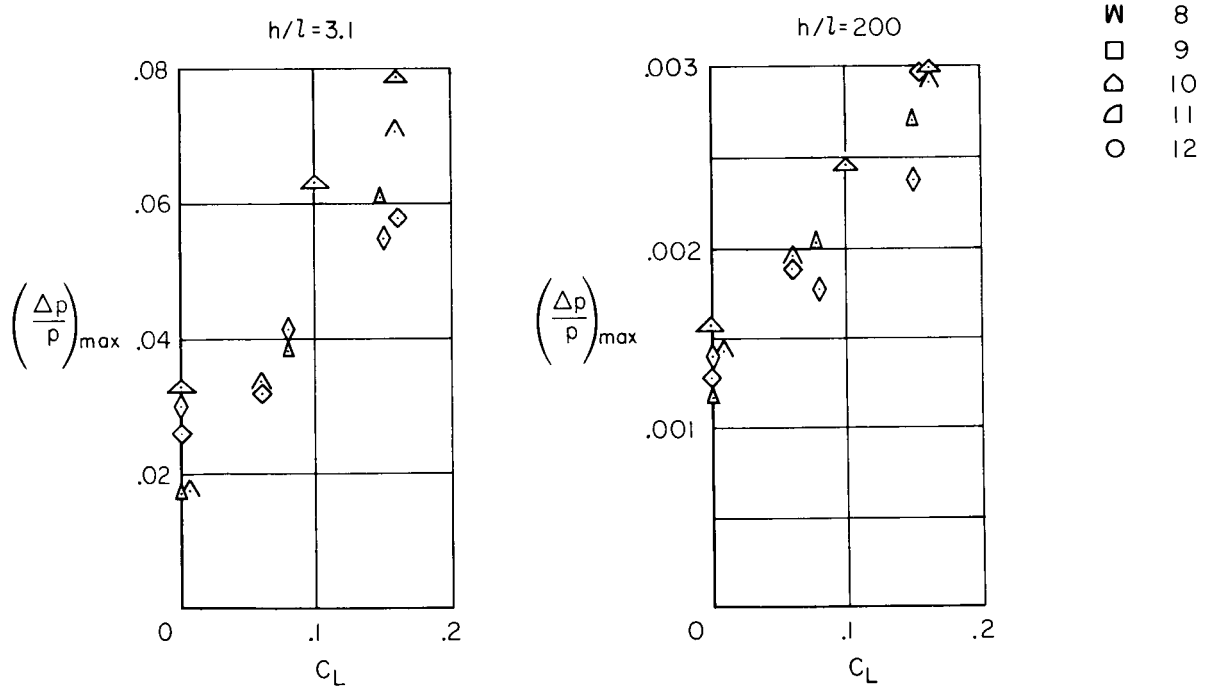

(b) M = 2.70

Figure 10.– Summary of maximum overpressure characteristics for the various models based on experimental data.

NASA-Langley, 1973 — 23 A–4491